3/4A

Continued Development of Earthquake Load and Resistance Factor Design Guidelines

Report 3

Benchmark Platform and Site Studies

by

Professor Robert Bea

and

James Stear

Marine Technology & Management Group

Department of Civil & Environmental Engineering

University of California at Berkeley

March 1999

Table of Contents

Appendix A Simplified Strength Level Earthquake Assessment of Jacket Type Platforms

Chapter 1

Introduction

1.0 Objective

The objective of this study is to continue development of earthquake load and resistance factor design (LRFD) guidelines as follows:

- Part 1 - concrete gravity based structure (GBS) LRFD guidelines (sponsored by Health and Safety Executive),
- Part 2 - seismic hazard characterizations (sponsored by STATOIL and UNOCAL) and
- Part 3 - verification of guidelines (sponsored by U. S. Minerals Management Service).

This report summarizes the results of the third part of this study; benchmark platform and site studies. Two primary topics are addressed:

- benchmark studies performed on 4 platforms to compare the proposed ISO guidelines with current API (1993) guidelines ; and
- benchmark studies performed on offshore locations to compare the proposed ISO guidelines design spectra with those from recent site – platform specific studies.

1.1 Background

A first-generation LRFD ISO guideline for design of steel, pile supported, template-type platforms to resist earthquake induced loading has been developed (Bea 1996; 1997a). This guideline was based on the API RP 2A LRFD guideline and on the collective experience and judgment of the ISO P5 committee members. During the first generation developments, limited verification studies of the entire process were performed, there was limited documentation of the background for some of the key developments, and there were additional topics that needed to be addressed. These topics have been discussed and the P5 committee recommended that additional studies be conducted on the three topics cited above.

The report titled *Continued Development of Earthquake Load and Resistance Factor Design Guidelines, Report 1 - Concrete Gravity Base Structures LRFD Guidelines* documented the results of the first phase of this study (Bea, 1998a).

The report titled *Continued Development of Earthquake Load and Resistance Factor Design Guidelines, Report 2 - Seismic Hazard Characterizations* documented the results of the second phase of this study (Bea, 1998b).

1.2 Earthquake LRFD Approach

The LRFD approach used to develop the proposed ISO earthquake design guidelines can be expressed analytically as follows:

$$\phi_E R_E \geq \gamma_{D1} D_1 + \gamma_{D2} D_2 + \gamma_{L1} L_1 + \gamma_E E$$

where ϕ_E is the resistance factor for earthquake loadings, R_E is the design capacity of the platform element (e.g. brace, joint, pile) for earthquake loadings as defined by the API RP 2A - LRFD guidelines, γ_{D1} is the self-weight of the structure (dead) loading factor, D_1 is the design dead loading, γ_{D2} is the imposed equipment and other objects loading factor, D_2 is the design equipment loading, γ_1 is the consumables, supplies, and vessel fluids (live) loading factor, L_1 is the live loading, γ_E is the earthquake loading factor, and E is the earthquake loading effect developed in the structure or foundation element. This development addresses the definition of the resistance factors, ϕ_E , and the loading factors, γ_E , for loadings induced by earthquakes (Bea, 1997a). The dead, equipment and live loading factors are set as $\gamma_{D1} = \gamma_{D2} = \gamma_{L1} = 1.1$.

The earthquake loading factor is determined using a Lognormal format (Bea, 1996):

$$\gamma_E = \mathbf{Fe}\, \mathbf{B_E} \exp (0.8\, \beta_E\, \sigma_E - 2.57\, \sigma_E)$$

where **Fe** is the median effective loading factor, $\mathbf{B_E}$ is the median bias (actual / nominal) in the computed earthquake loadings, β_E is the annual Safety Index designated for the platform SSL, σ_E is the total uncertainty associated with the earthquake loadings (standard deviation of the annual maximum earthquake loading), 0.8 is the splitting factor used to separate the uncertainties in earthquake loadings and platform capacities, and the 2.57 is a consequence of defining the elastic design earthquake (Strength Level Earthquake) at an average return period of 200-years (2.57 Standard Normal deviations from the mean).

The effective loading factor for the platform system is expressed as:

$$\mathbf{Fe} = [\, \mu\, \alpha\,]^{-1}$$

where μ is the platform system ductility and α is the platform residual strength ratio:

$$\mu = \Delta p / \Delta e$$

$$\alpha = A / Aep$$

Δp is the maximum plastic displacement that can be developed by the platform system at 'failure', Δe is the displacement at which first significant nonlinear behavior is indicated by the platform system, A is the area under the platform loading - displacement to failure diagram, and Aep is the area under an equivalent elasto-plastic platform loading - displacement to failure diagram.

The total uncertainty associated with the earthquake loadings (σ_E) is expressed as:

$$\sigma_E^2 = \sigma_{SE}^2 + \sigma_{GS}^2 + \sigma_{RS}^2$$

where σ_{SE} is the uncertainty in the earthquake horizontal peak ground accelerations, σ_{GS} is the uncertainty related to the local geology and soil conditions and their effects on the ordinates of the earthquake response spectra, and σ_{RS} is the uncertainty associated with the response spectrum method used to determine forces in the elements that comprise the platform.

In development of the proposed ISO earthquake guidelines, Type I (natural, inherent, aleatory) uncertainties are included in σ. The effects of Type II (model, parameter, state, epistemic) uncertainties are introduced with the Biases (actual value / nominal value) in loading effects and

capacities. This is done to develop as close as possible a correlation with the way in which the target Safety Indices and probabilities of failure were determined.

The platform element resistance factor is determined from:

$$\phi_E = \mathbf{B}_{RE} \exp(-0.8\,\beta_E\,\sigma_{RE})$$

where $\mathbf{B}_{RE}$ is the median bias (actual value / nominal or code value) in the element earthquake loading capacity, and is the σ_{RE} uncertainty in the earthquake loading capacity of the element .

The proposed ISO earthquake LRFD approach proceeds through the following nine steps (Bea 1997a):

1) Define the structure safety and serviceability level (SSL)
2) Define the earthquake hazard zone (EHZ) and seismotectonic conditions (Figure 1.1)
3) Determine if site specific seismic exposure study is required (Table 1.1)
4) Define the shape of the normalized mean elastic principal horizontal acceleration response spectrum for a specified damping ratio, soil profile, and seismotectonic condition (Figure 1.2, Table 1.2)
5) Determine the uncertainties associated with the seismic exposure, response spectrum, and the methods used to analyze earthquake forces induced in the structure (Table 1.3, Table 1.4)
6) Determine the earthquake loading factor (γ_E) for the elastic response spectra forces (Figure 1.3)
7) Evaluate the biases and uncertainties in the platform element design capacities
8) Determine if a ductility analysis is required and the performance characteristics for the analyses
9) Determine the platform element resistance factors (ϕ_E) for the design code based capacities (Figure 1.4)

The remainder of this report will summarize the benchmark study of four platforms to compare the proposed ISO guideline based earthquake induced forces with those determined using the current API guidelines. In addition, benchmark studies will be performed on results from XX sites to compare the proposed ISO design spectra with current site and platform specific spectra. Given that the proposed ISO response spectra based force guidelines have not deviated from the API guidelines, such comparisons should provide direct comparisons of the Strength Level design forces induced in the platforms.

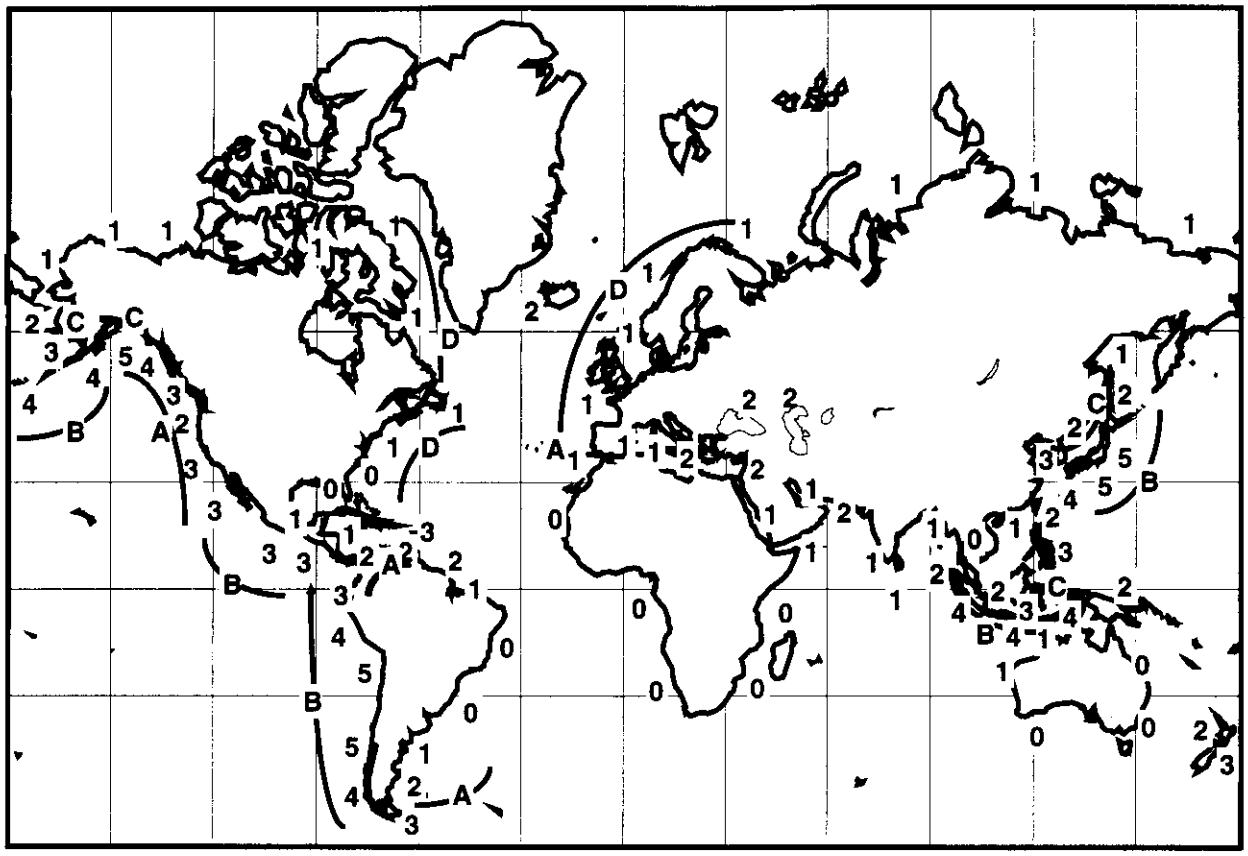

Figure 1.1 - Proposed ISO Earthquake Hazard Zones (EHZ)

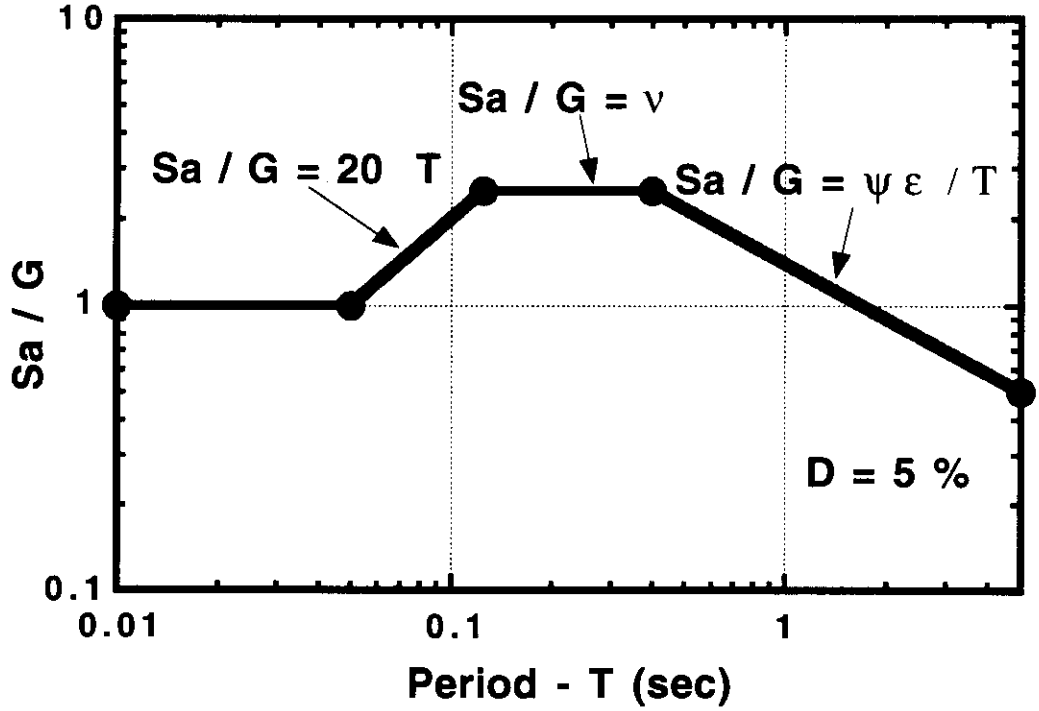

Figure 1.2: Proposed ISO elastic design response spectra

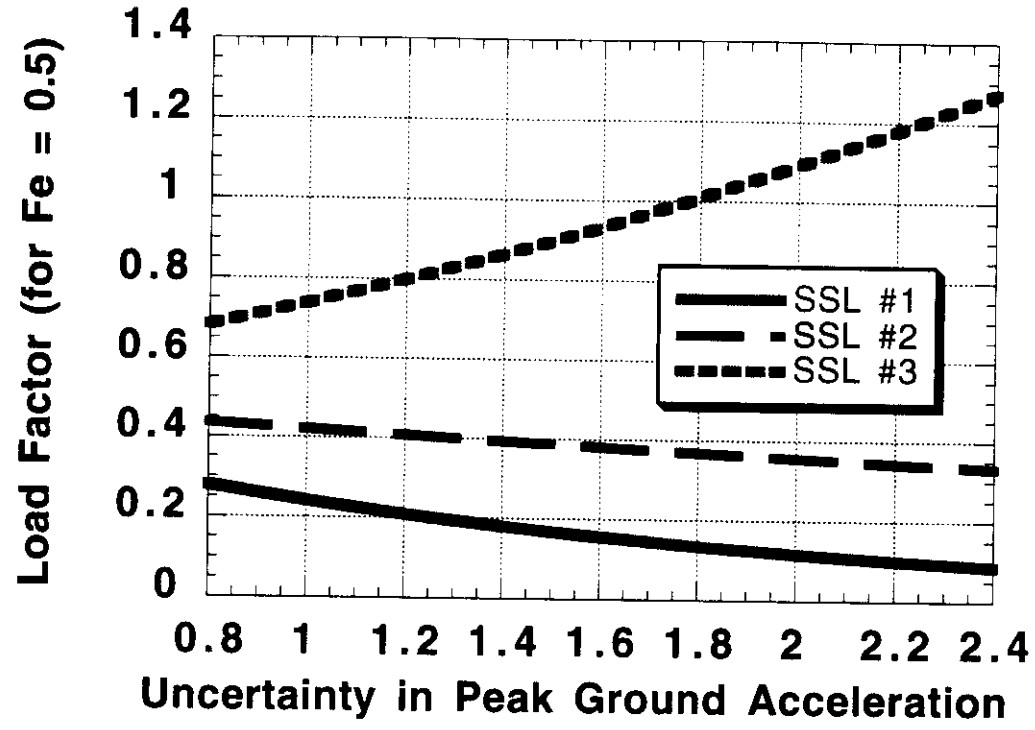

Figure 1.3: Earthquake loading factors

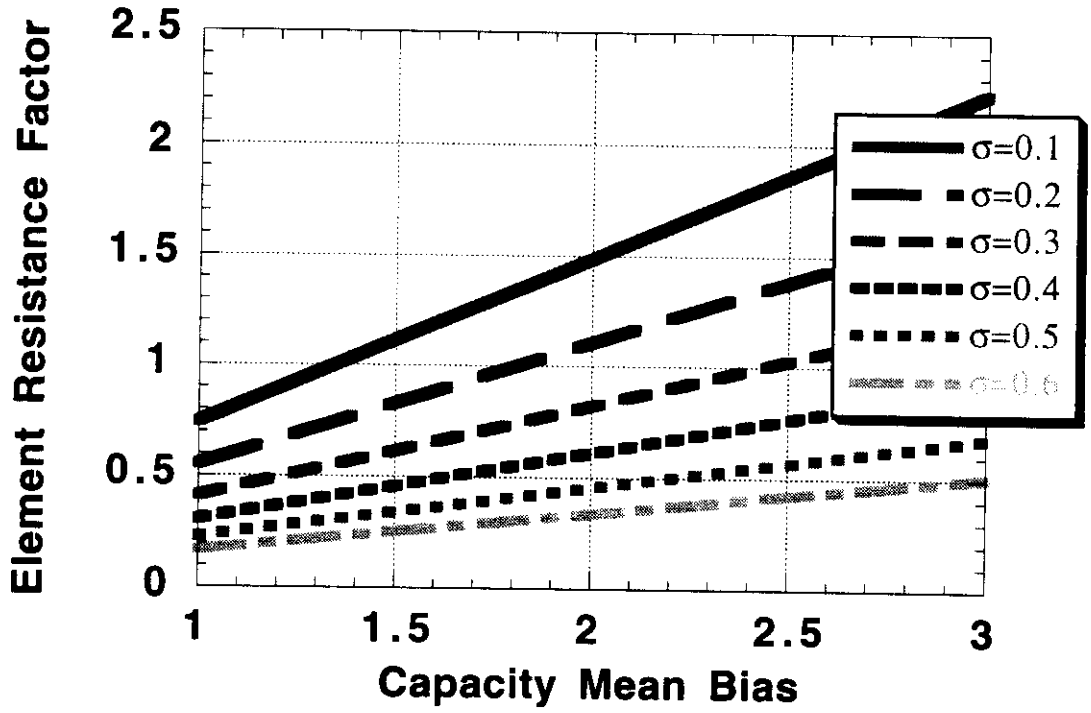

Figure 1.4: Platform element resistance factors (for SSL 3)

Table 1.1: Proposed ISO Earthquake Hazard Zones, SLE Ground Accelerations (G) and Structural Serviceability & Safety Levels (SSL)

Zone (1)	SLE G % g (2)	SSL #1 (3)	SSL #2 (4)	SSL #3 (5)	SSL #4 (6)
0	0 - 5	Allowed to use these guidelines		Should do site specific study	MUST DO SITE SPECIFIC STUDY
1	5 -15				
2	15 -25				
3	25 -35				
4	35 -45				
5	45 -55				

Table 1.2: Local geology and soil conditions parameters for SLE response spectra

Soil Conditions			Seismotectonic Conditions	
Site Class	ν	ψ		ε
SC-A	2.5	1.0	Type A	1.0
SC-B	3.3	1.2	Type B	0.8
SC-C	3.5	1.4	Type C	0.9
SC-D	4.5	2.0	Type D	0.8
SC-E	Site specific studies required		Default value	1.0

Table 1.3: Seismic sources and attenuation uncertainties

Seismotectonic Characteristics	σ_{SE}
Shallow crustal fault zones	1.0
Deep subduction zones	1.4
Mixed shallow crustal fault and deep subduction zones	1.2
Intraplate zones	2.0

Table 1.4: Uncertainties associated with local geology and soil conditions

Geology / Soil Conditions	σ_{GS}
SC - A	0.30
SC - B	0.40
SC - C	0.40
SC - D	0.50
SC - E	0.50

Chapter 2

Benchmark Platform Studies

2.0 Introduction

In the following examples, the ISO spectra have been used to generate earthquake lateral loadings and capacities for four jacket-type platforms located off the Southern California coast. These loads are compared to loads generated through application of the API RP 2A-WSD (1993) design response spectra. The goal of these analyses is to demonstrate how both sets of spectra compare, given the same set of generic definition parameters, and to study the relative conservatism of the ISO spectra with regards to the API spectra.

The computer program TOPCAT (Stear, Bea, 1998a) is used to perform the analyses. This program incorporates a response spectra based method to determine the earthquake forces induced in platforms. The program has been verified with results from full three-dimensional linear and nonlinear computer programs. The program has been demonstrated to produce earthquake loadings and platform capacities very close to those determined using the more complex programs (Stear, Bea, 1998b; Stear, Bea, 1999).

The formulations for the TOPCAT response spectra analyses and platform capacity analyses are summarized in Appendix A. Appendix A also documents the verifications of the TOPCAT seismic loading analyses.

2.1 Platform A

Platform A is a design for a symmetric 4-leg production platform (Figure 2.1). The structure is designed for 100 ft water depth. The deck is at +50 ft MWL and supports a load of 5,000 kips. The main diagonals in the first jacket bay are 24 inch-diameter (w.t. 0.5 inch), while those in the second bay are 30 inch-diameter (w.t. 0.625 inch); the diagonals in the deck bay are 36 inch-diameter (w.t. 0.75 inch). The joints into which the braces are framed are heavy-wall joint cans. The legs are 78 inch-diameter (w.t. 0.875 to 1.125 inches); the annulus between each leg and associated pile is grouted. The piles are 72 inch-diameter (w.t. 1 to 1.5 inches), and are designed for 150 ft penetration in medium to stiff clay. The shear strength of the clay is 2.5 kips/ft^2 at the surface, and increases by 0.01 kip/ft^2 per ft of depth. The pile ends are founded on a very stiff soil layer (rock) which has a shear strength of 184 kips/ft^2. All steel in the jacket is 36 ksi, while the pile steel is 50 ksi. The platform has a fundamental lateral period of 1.52 sec.

Platform A is founded on soils categorized as stiff to very stiff overlying rock, and the seismotectonic conditions are described as shallow crustal faulting. Hence, the platform has been assessed using both the API Soil B response spectrum and the ISO spectrum with $\nu = 3.3$, $\Psi = 1.2$ and $\varepsilon = 1.0$. The two response spectra are shown in Figure 2.2; horizontal demand-capacity curves

developed using the two spectra each scaled to a zero period acceleration (ZPA) of 0.5 g are shown in Figures 2.3 and 2.4.

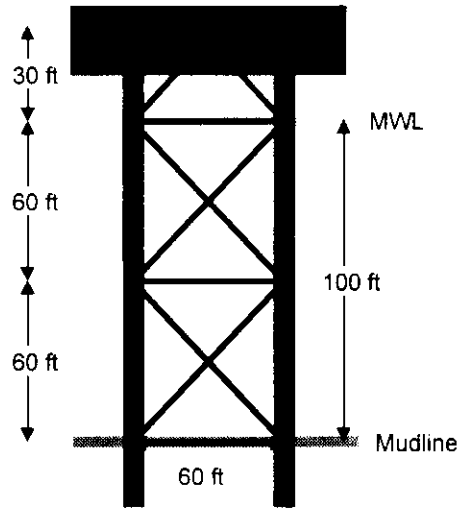

Figure 2.1: Platform A

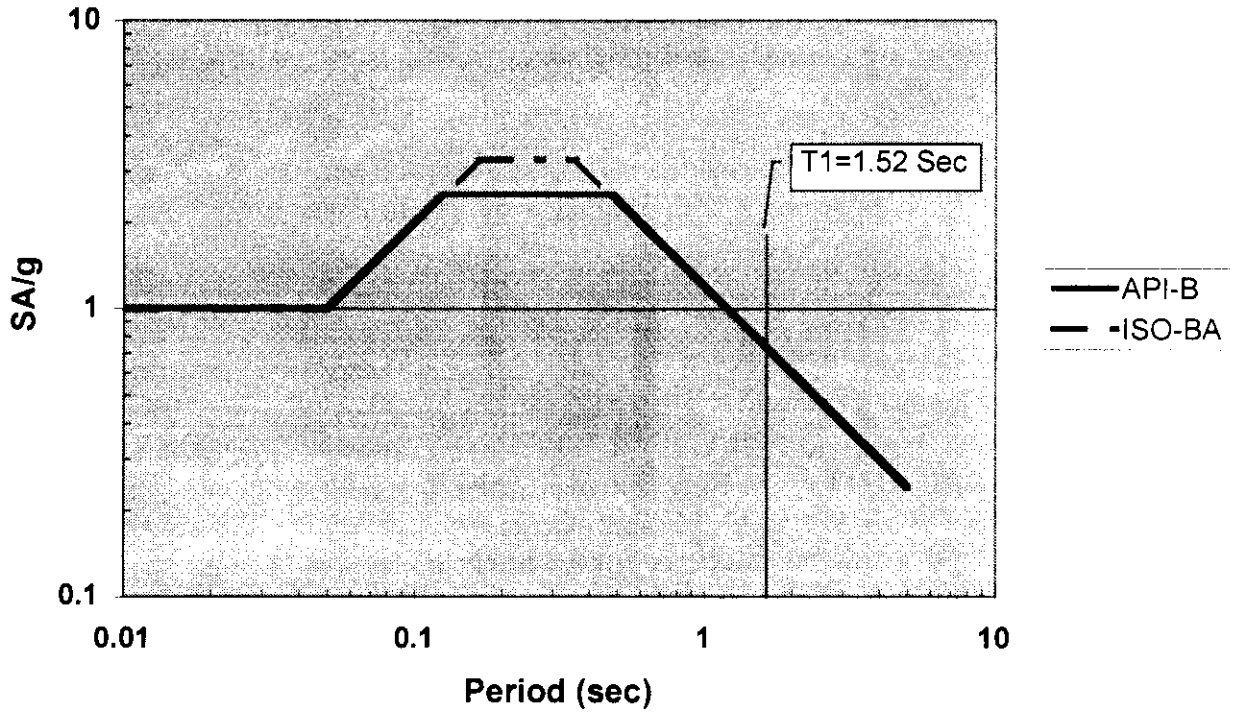

Figure 2.2: API and ISO Response Spectra

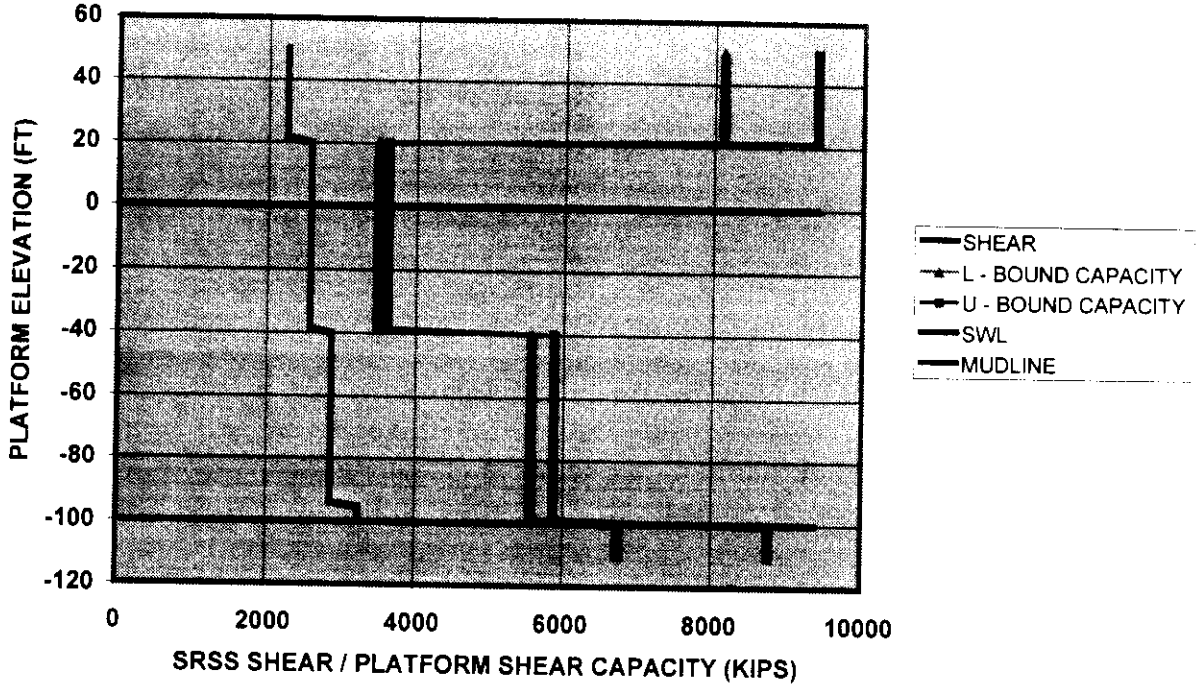

Figure 2.3: Platform A Demand-Capacity, API Soil B ZPA=0.5 g

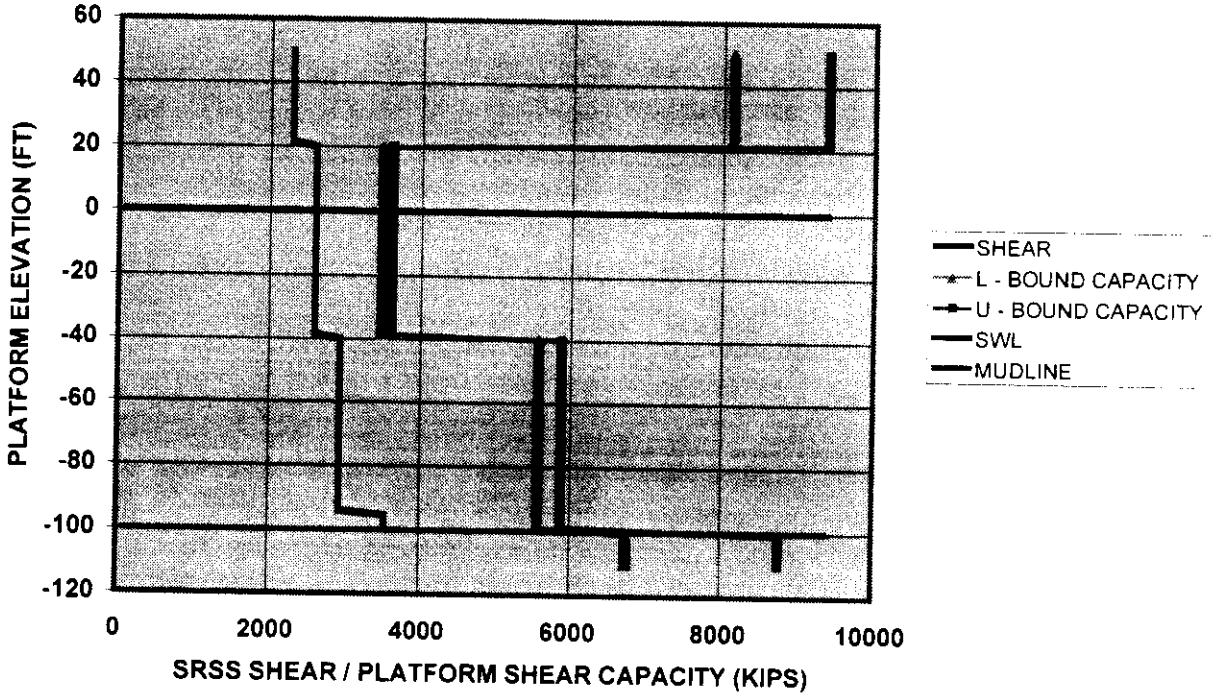

Figure 2.4: Platform A Demand-Capacity, ISO Site B, Seismotectonic A ZPA=0.5 g

Horizontal and vertical earthquake loads on the platform were determined using the SRSS modal combination rule. Vertical excitation was scaled to a ZPA equal to one-half that used for horizontal excitation.

Given the similarity in spectral shapes in the period range of interest, it is not surprising that the shear demand profiles generated by their application are nearly identical. The strength limit state of the platform is exceeded for a spectrum intensity, expressed by ZPA, of 0.67 g for both the API and ISO load cases. The platform capacity is governed by the strength of the diagonal braces in the first jacket bay.

2.2 Platform B

Platform B is an 8-leg drilling platform sited in 265 ft of water in San Pedro Bay off Southern California (Figure 2.5). It was designed to support 80 24 inch-diameter conductors. The platform has two decks located at +45 ft MWL and +64 ft MWL respectively; the deck bay is braced. The jacket is battered 1:7 in the broadside direction, and 1:12 in the end-on direction. The main diagonals range from 20 inch-diameter (w.t. 0.75 inch) to 36 inch-diameter (w.t. 1.125 inches). The corner legs of the jacket are 71 inch-diameter (w.t. 1 to 2 inches), while the interior legs are 54 inch-diameter (w.t. 0.675 to 2 inches); the legs have heavy joint cans but are not grouted. The corner piles of the platform are 66 inch-diameter, and penetrate to 264 ft. The center piles are 48 inch-diameter, and penetrate to 232 ft. The soil at the site is predominantly clay (medium-stiff to stiff). The majority of the structural members are 36 ksi steel, while the piles are 50 ksi steel. The end-on fundamental period of vibration is 2.59 sec, while the broadside fundamental period is 2.49 sec.

Platform B is founded on soils categorized as moderately stiff, and the seismotectonic conditions are described as shallow crustal faulting. Hence, the platform has been assessed using both the API Soil C response spectrum and the ISO spectrum with $\nu = 3.5$, $\Psi = 1.4$ and $\varepsilon = 1.0$. The two response spectra are shown below in Figure 7. The ISO spectrum developed assuming Site Class C results in spectral accelerations which are less than the API Soil C spectrum. For comparison purposes, the ISO spectrum assuming Site Class D is also shown; this provides spectral accelerations which are closer to those obtained from the API Soil C spectrum.

Horizontal demand-capacity curves have been developed using the two spectra (each scaled to a ZPA of 0.25 g) and are shown in Figures 2.7 and 2.8 for the case of broadside excitation. Horizontal and vertical earthquake loads on the platform were determined using the SRSS modal combination rule. Load components were scaled according to the following: primary horizontal = 100%, secondary horizontal = 67%, vertical = 50%.

Loads estimated from the ISO spectrum with the parameters listed above are in the range of 10% to 15% below those estimated from using the API spectrum. The strength limit state of the platform is exceeded for an intensity of 0.34 g (end-on axis as primary) using the API spectrum and an intensity of 0.38 g (end-on axis as primary) using the ISO spectrum. Platform capacity in both cases was governed by the yielding of a corner pile in compression.

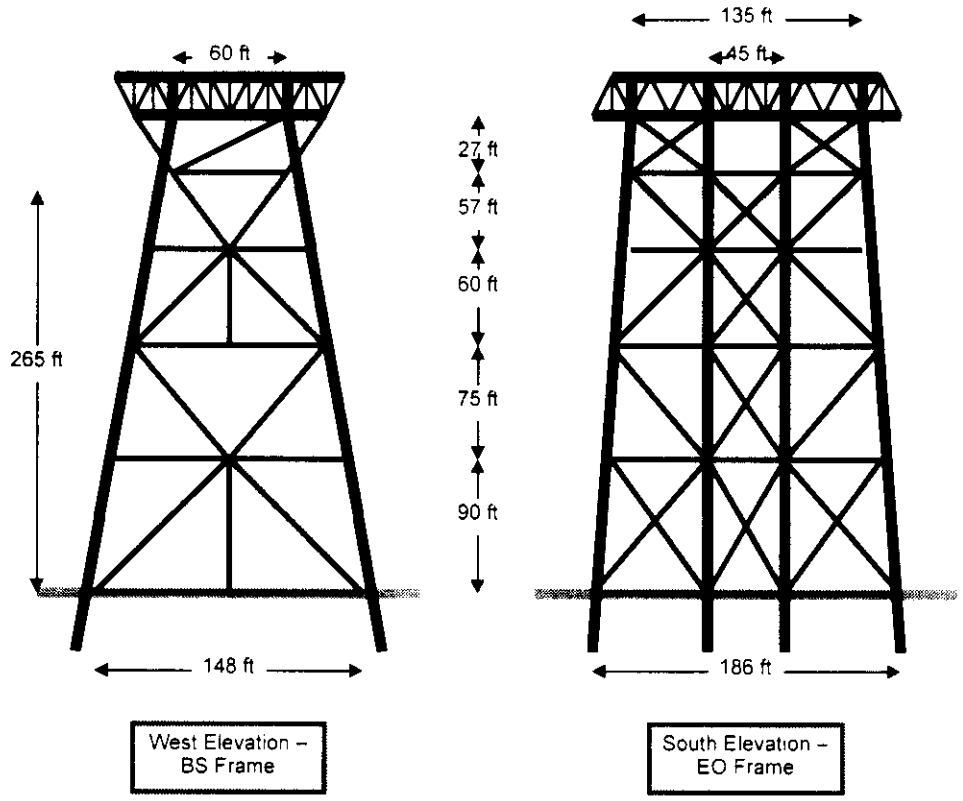

Figure 2.5: Platform B

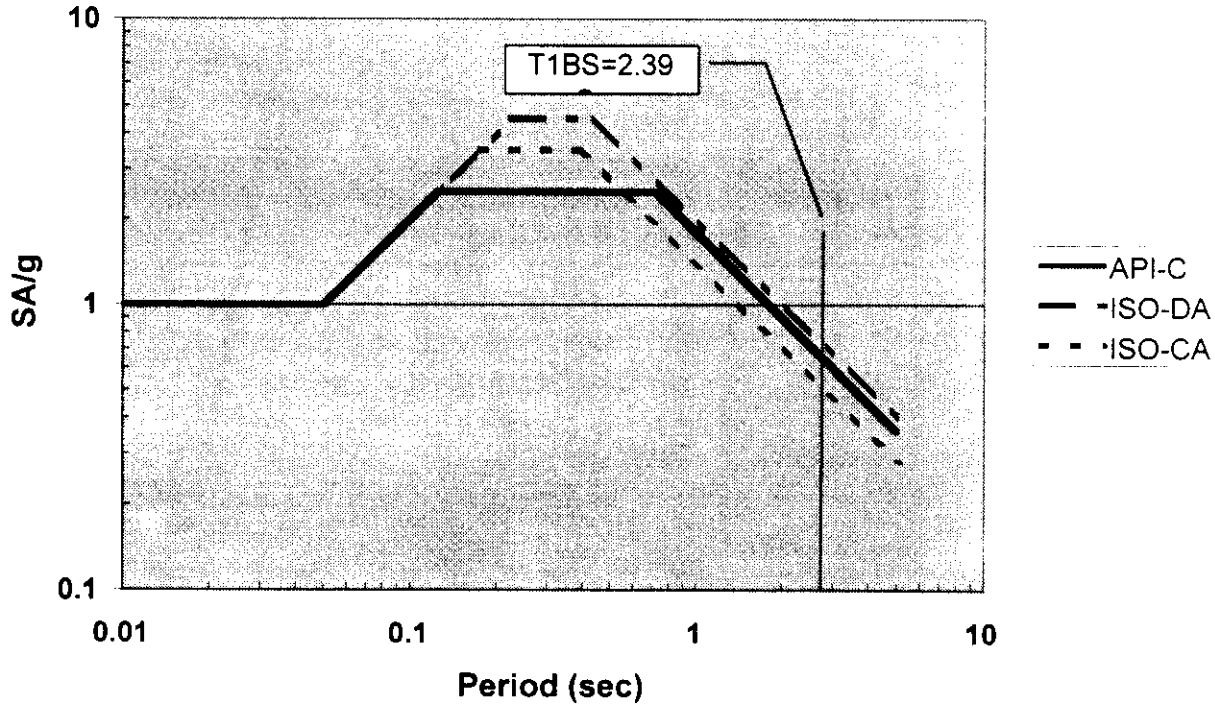

Figure 2.6: API and ISO Response Spectra

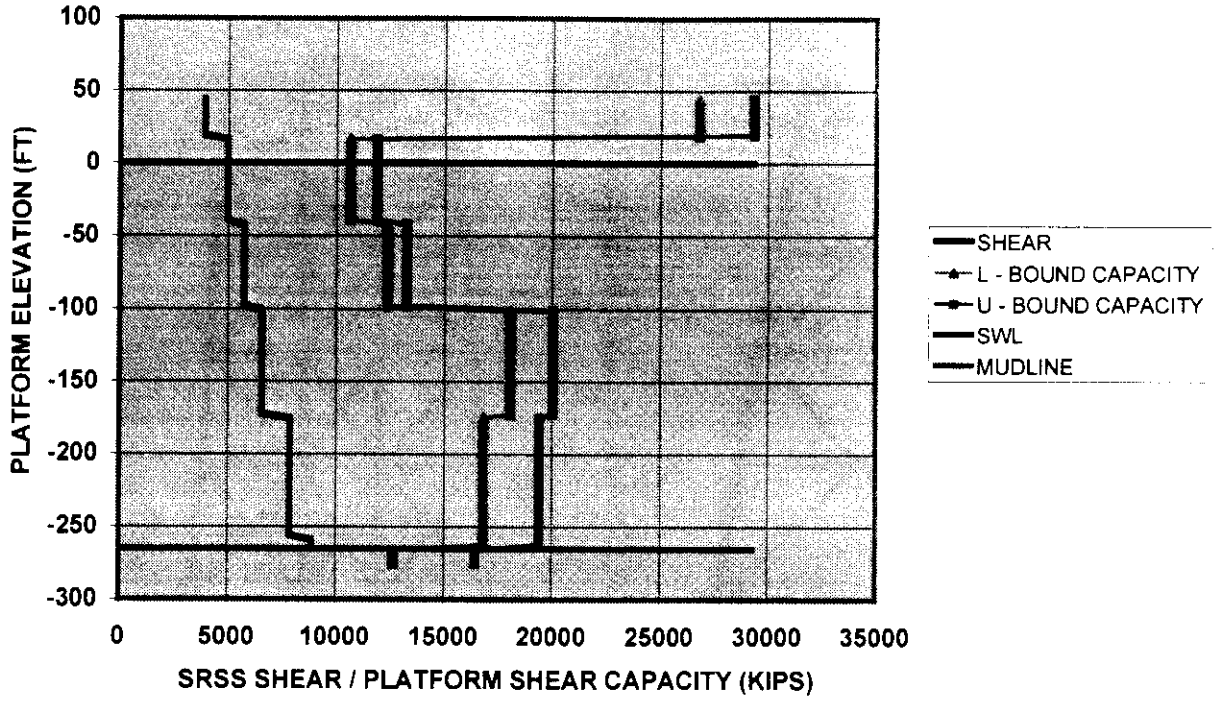

Figure 2.7: Platform B Broadside Demand-Capacity, API Soil C ZPA=0.25 g

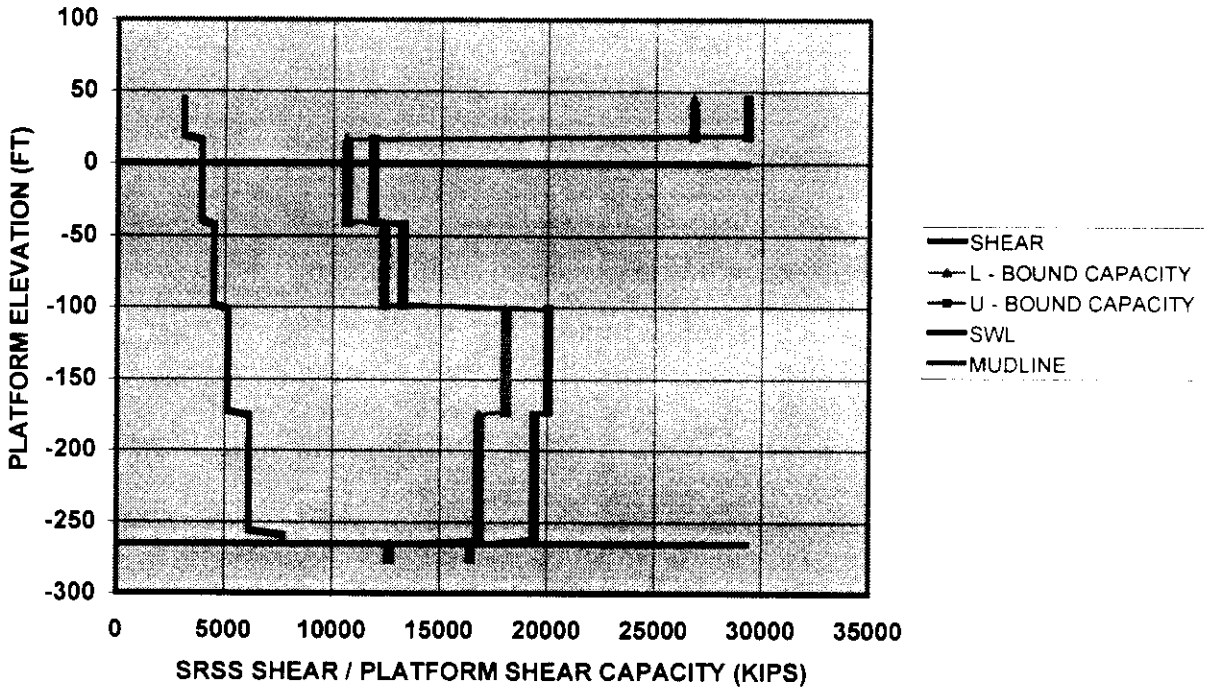

Figure 2.8: Platform B Broadside Demand-Capacity, ISO Site C, Seismotectonic A ZPA=0.25 g

2.3 Platform C

Platform C is a 12-leg production platform sited in 257 ft of water in San Pedro Bay off Southern California (Figure 2.9). The platform has two decks located at +45 ft MWL and +71 ft MWL respectively; the deck bay is braced. The jacket is battered 1:10 in the broadside direction, and 1:14 in the end-on direction. The main diagonals range from 24 inch-diameter (w.t. 0.625 inch) to 36 inch-diameter (w.t. 0.75 inches). The exterior legs of the jacket are 53 to 54 inch-diameter (w.t. 0.75 to 1 inch), while the two interior legs are 47 inch-diameter (w.t. 0.675 to 1 inch); the legs have heavy joint cans but are not grouted. The exterior piles of the platform are 48 inch-diameter; the corners penetrate to 252 ft, while the remainder penetrate to 221 ft. The interior piles are 42 inch-diameter, and penetrate to 200 ft. The soil profile at the site is the same as for Platform B. The majority of the structural members are 36 ksi steel, while the piles are 42 ksi steel. The platform has an end-on fundamental period of 2.02 sec, and a broadside fundamental period of 2.09 sec.

Platform C is founded on soils categorized as moderately stiff, and the seismotectonic conditions are described as shallow crustal faulting. Hence, the platform has been assessed using both the API Soil C response spectrum and the ISO spectrum with $\nu = 3.5$, $\Psi = 1.4$ and $\varepsilon = 1.0$. The two response spectra are shown below in Figure 2.10. The ISO spectrum developed assuming Site Class C results in spectral accelerations which are less than the API Soil C spectrum. For comparison purposes, the ISO spectrum assuming Site Class D is also shown; this provides spectral accelerations which are closer to those obtained from the API Soil C spectrum.

Horizontal demand-capacity curves have been developed using the two spectra (each scaled to a ZPA of 0.25 g) and are shown in Figures 2.11 and 2.12 for the case of end-on excitation. Horizontal and vertical earthquake loads on the platform were determined using the SRSS modal combination rule. Load components were scaled according to the following: primary horizontal = 100%, secondary horizontal = 67%, vertical = 50%.

Loads estimated from the ISO spectrum with the parameters listed above are in the range of 8% to 12% below those estimated from using the API spectrum. The strength limit state of the platform is exceeded for an intensity of 0.27 g (end-on axis as primary) using the API spectrum and an intensity of 0.31 g (end-on axis as primary) using the ISO spectrum. Platform capacity in both cases was governed by the formation of hinges in the piles.

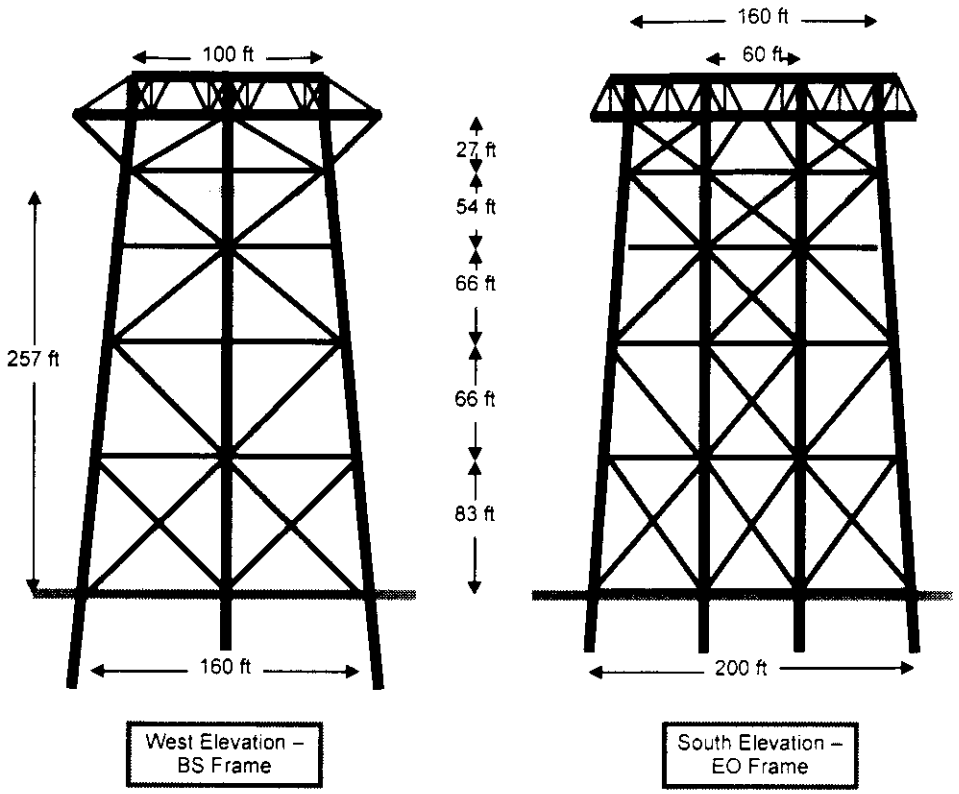

Figure 2.9: Platform C

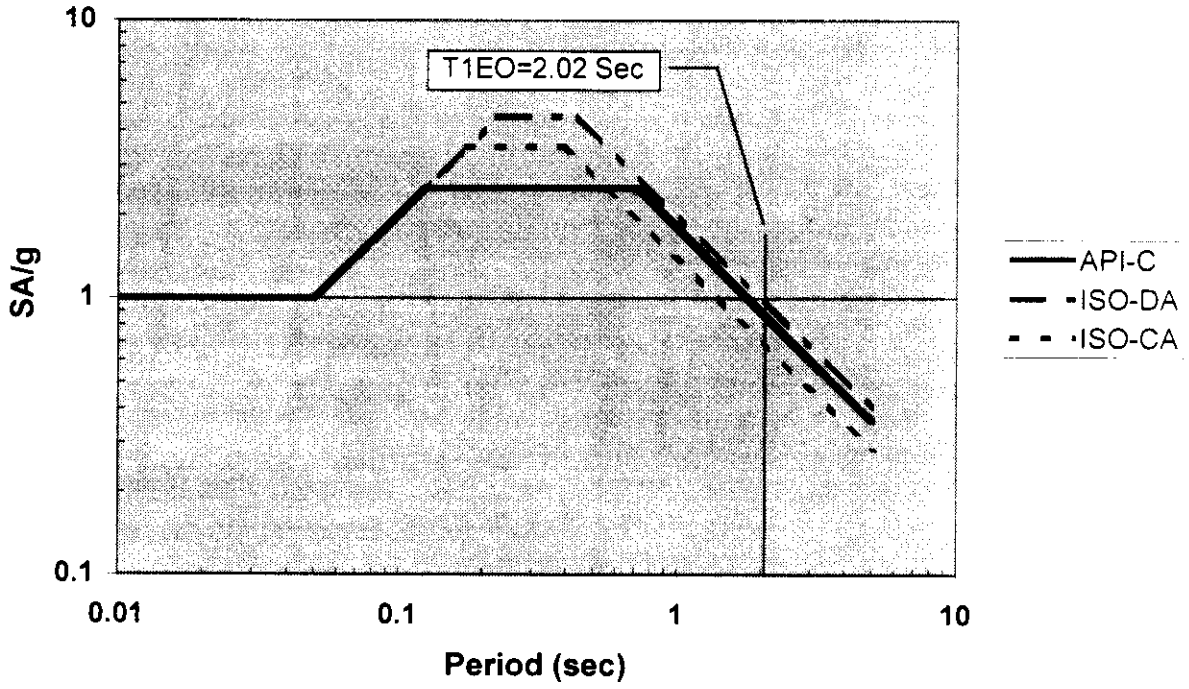

Figure 2.10: API and ISO Response Spectra

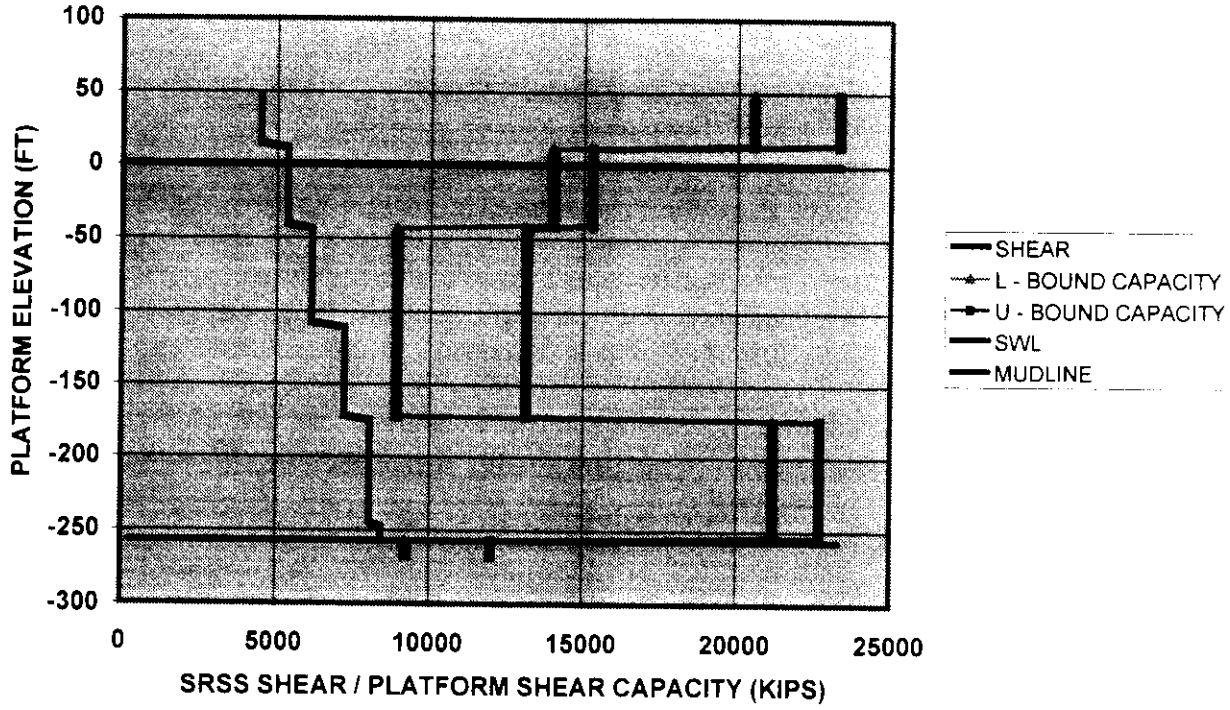

Figure 2.11: Platform C End-On Demand-Capacity, API Soil C ZPA=0.25 g

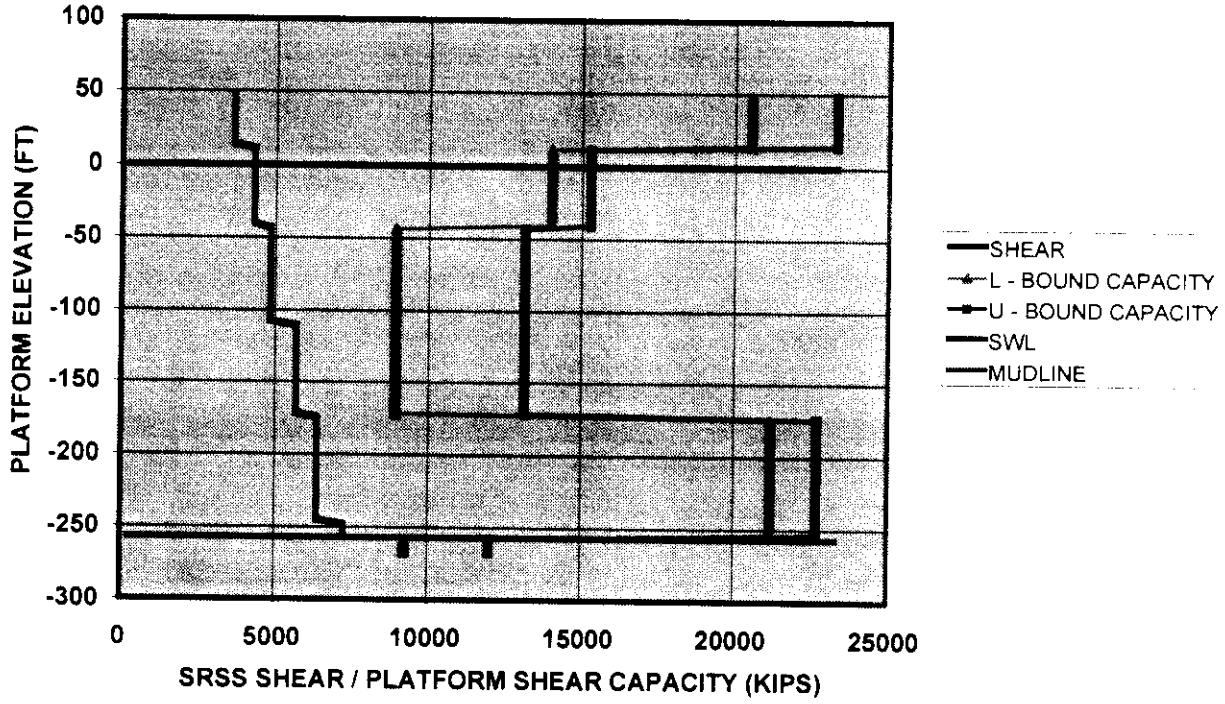

Figure 2.12: Platform C End-On Demand-Capacity, ISO Site C, Seismotectonic A ZPA=0.25 g

2.4 Platform D

Platform D is a 12-leg drilling and production platform sited in 58 ft of water off Huntington Beach in Southern California (Figure 2.13). The platform supports 42 20 inch-diameter conductors, 12 of which are guided at the mudline and can be expected to provide lateral resistance. The platform has two decks located at +34 ft and +58 ft respectively. There is minimal diagonal bracing between the decks and between the decks and the jacket. The main diagonals in the jacket range from 12 inch-diameter (w.t. 0.33 inch) to 14 inch-diameter (w.t. 0.375 inch). The jacket legs are 33 inch-diameter; the jacket legs possess 18 ft extensions which penetrate into the foundation soil. The annulus between each leg and associated pile is grouted. The piles are 30 inch-diameter (w.t. 0.875 to 1.5 inches), and penetrate between 60 to 80 ft through layers of silt, clay and sand. All steel is assumed to be 36 ksi, with 10% increases taken for strain rate effects and correction from minimum specified strength to mean strength. The end-on fundamental period is 1.02 sec, while the broadside fundamental period is 0.97 sec.

Platform D has been assessed using both the API Soil A response spectrum and the ISO spectrum with $\nu = 2.5$, $\Psi = 1.0$ and $\varepsilon = 1.0$. These spectra were chosen as they provided the closest fit to a site-specific response spectrum which was developed previously for the platform's location. The two response spectra are shown below in Figure 2.14. Horizontal demand-capacity curves have been developed using the two spectra (each scaled to a ZPA of 0.25 g) and are shown in Figures 2.15 and 2.16 for the case of broadside excitation. Horizontal and vertical earthquake loads on the platform were determined using the SRSS modal combination rule. Load components were scaled according to the following: primary horizontal = 100%, secondary horizontal = 100%, vertical = 50%.

Loads estimated from the ISO spectrum with the parameters cited are in the range of 8% to 10% above those estimated from using the API spectrum. The strength limit state of the platform is exceeded for an intensity of 0.43 g using the API spectrum and an intensity of 0.38 g using the ISO spectrum. Platform capacity in both cases was governed by the failure of K-joints in the bottom broadside frames.

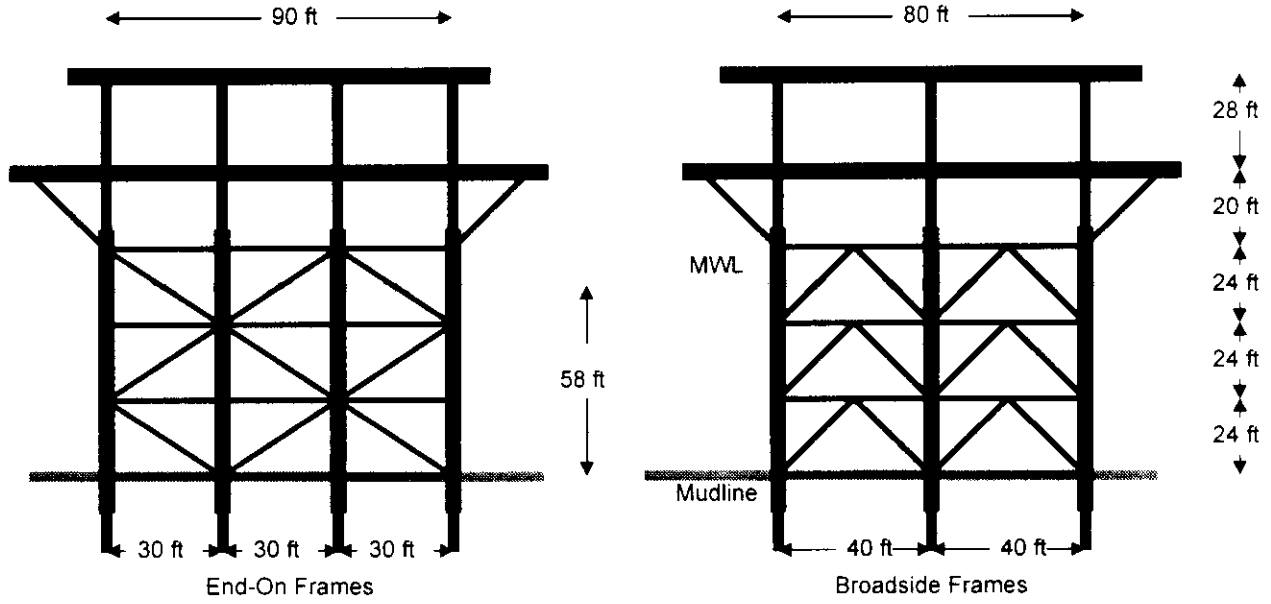

Figure 2.13: Platform D

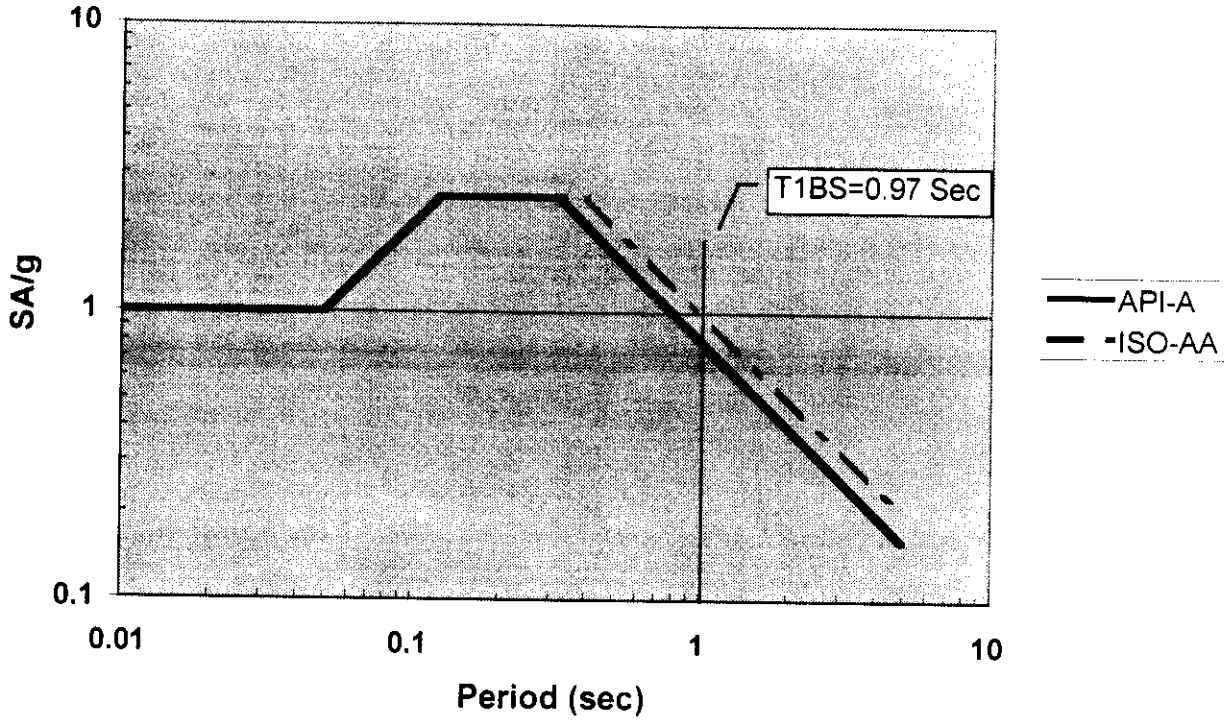

Figure 2.14: API and ISO Response Spectra

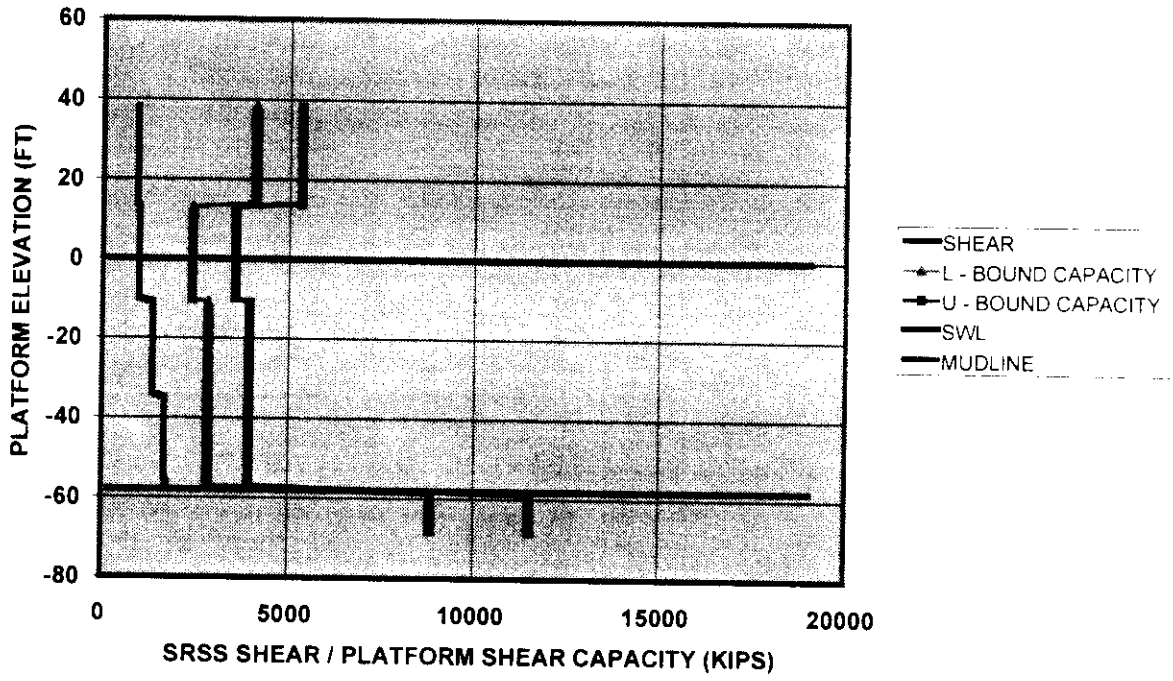

Figure 2.15: Platform D Broadside Demand-Capacity, API Soil A ZPA=0.25 g

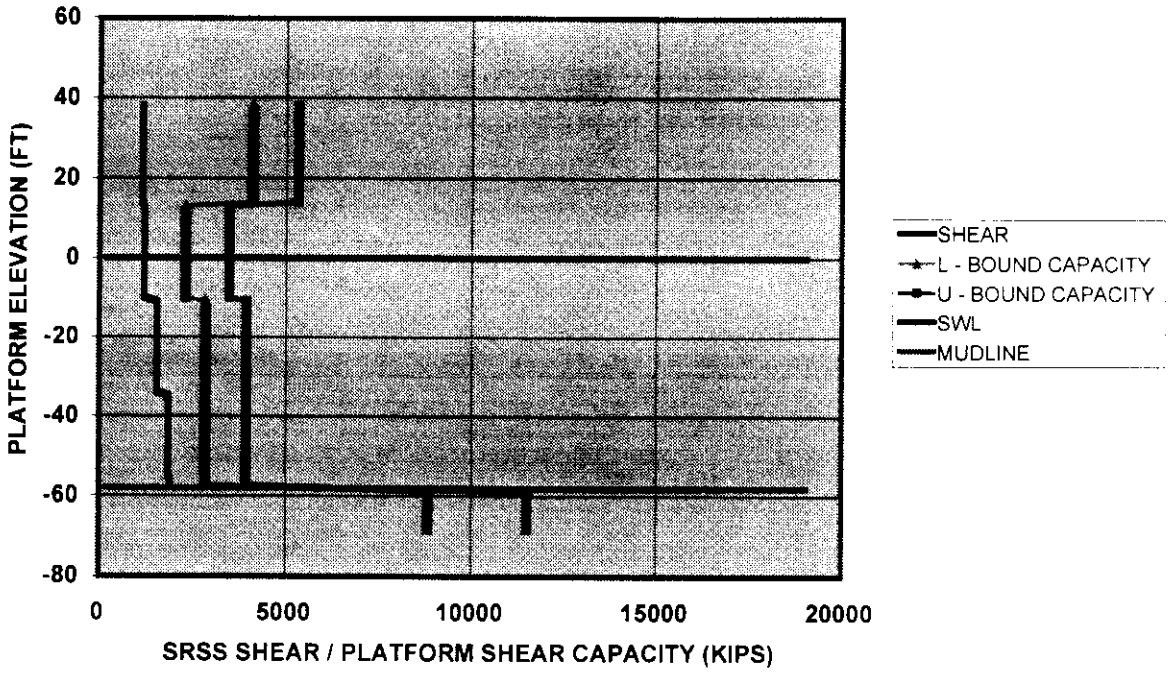

Figure 2.16: Platform D Broadside Demand-Capacity, ISO Site A, Seismotectonic A ZPA=0.25 g

2.5 Summary

The proposed ISO spectra provide loads which compare very well with loads generated using the API spectra over the period range covered by the four example platforms, indicating consistency between the two when site soil and seismotectonic conditions are similar.

Chapter 3

Benchmark Site Specific Spectra Studies

3.0 Introduction

Results from recent site – region specific seismic exposure studies in which site specific Strength Level Earthquake (SLE) design spectra were developed are compared with the proposed ISO SLE spectra. Results are developed for the U. K. and Norwegian Sectors of the North Sea, including the British Petroleum Gyda platform location. Site specific spectra are also studied for locations offshore Indonesia and New Zealand.

3.1 North Sea Regional SLE Response Spectra

SLE response spectra for North Sea seismotectonic and hard ground - rock conditions were developed as part of the EQE study of the UK Sector (1998) and the NORSAR study of the Norwegian Sector (1998). Figure 3.1 summarizes the normalized response spectra results for a 5 % damping ratio from the EQE study for return periods of 100 years, 1,000 years, and 10,000 years. The response spectra do not vary significantly as a function of the intensity of the earthquakes in this range. This is to be expected since the hard ground - rock materials respond essentially in their low-strain, reasonably elastic, range. The peak amplification of the spectra is approximately 2.5.

Figure 3.2 summarizes the response spectra from the NORSAR study (1998) for a return period of 10,000 years at low seismic activity (Alta) and high seismic activity (Midgard) sites for rock or hard ground conditions. The shapes of the spectra are essentially identical.

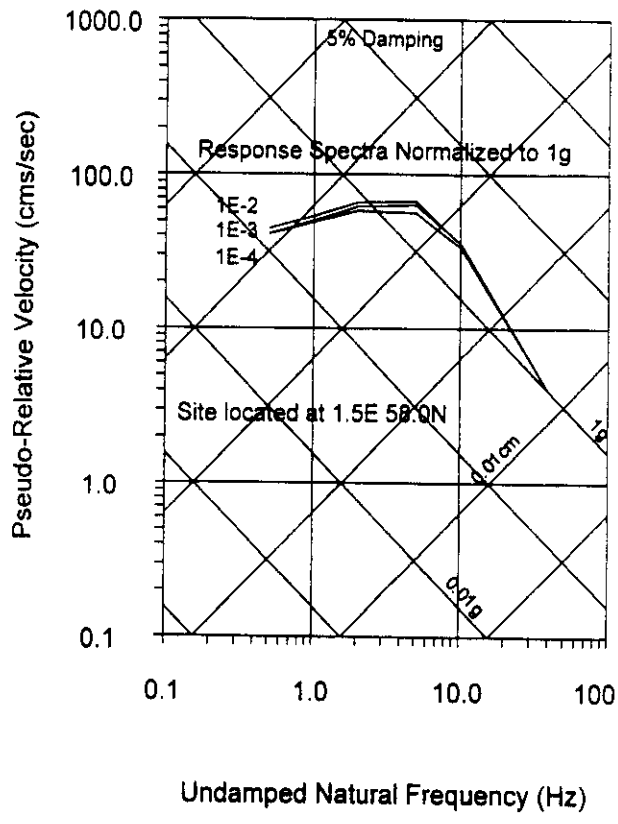

Figure 3.1: Earthquake Response Spectra for UK Sector Conditions

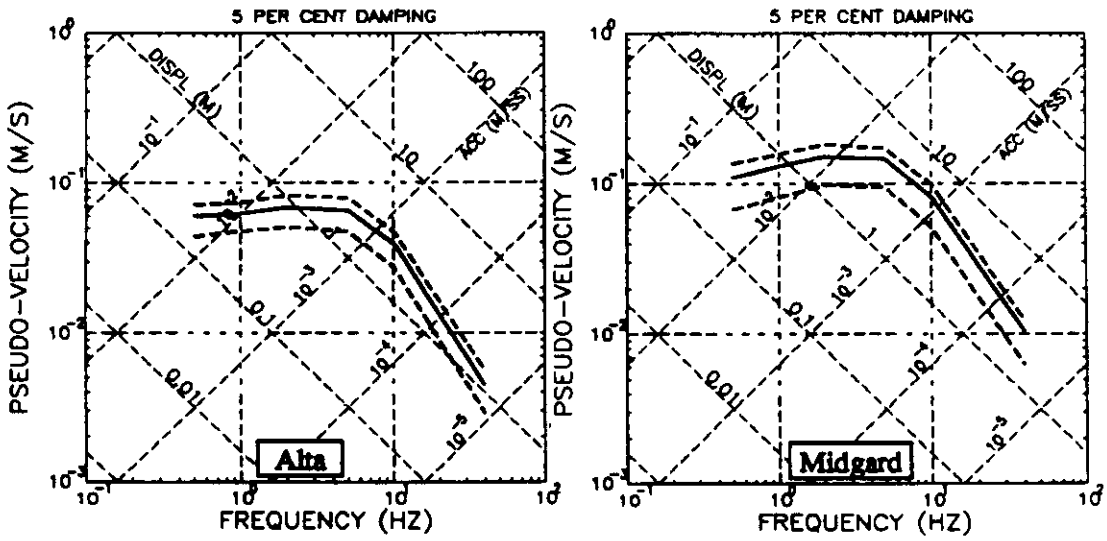

Figure 3.2: Earthquake Response Spectra for Norwegian Sector Conditions For Earthquake Return Period of 10,000 years and Rock - Hard Ground

Figure 3.3 compares the proposed ISO rock and UK – Norwegian sector SLE (200 year) spectra. The ISO spectra are more conservative than the UK – Norwegian sector spectra. The comparison for the UK and Norwegian sectors was based on the most intense ZPA in each of the sectors.

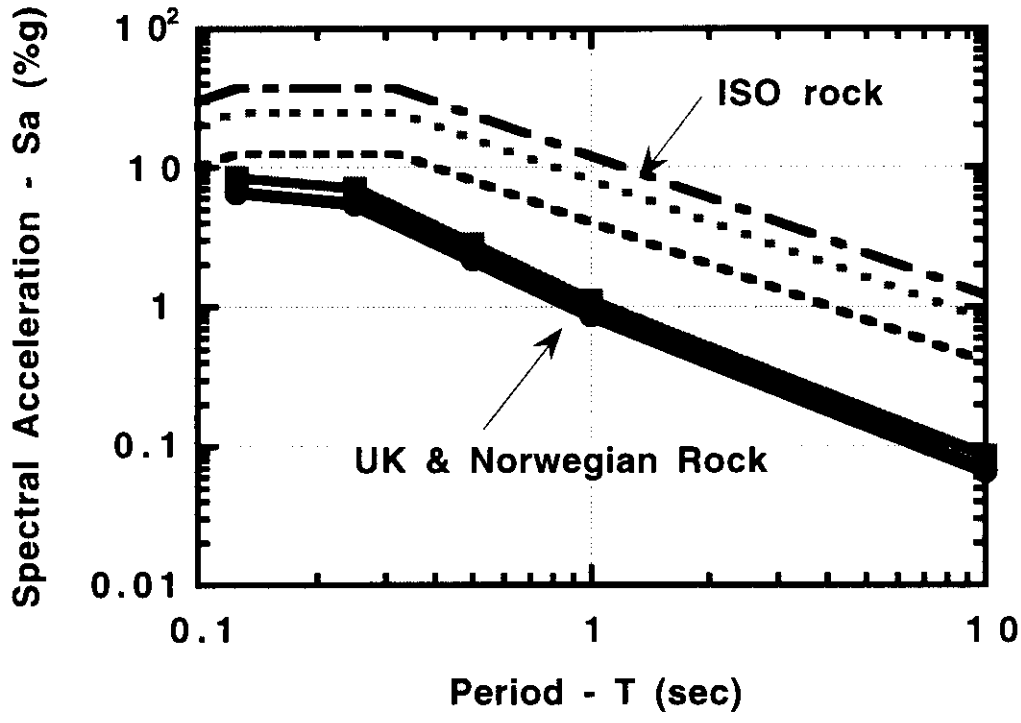

Figure 3.3: Comparison of proposed ISO and UK – Norwegian Sectors SLE Rock Spectra

Figure 3.4 and Figure 3.5 summarize results from the study of soil column effects on the rock spectra performed by the Norwegian Geotechnical Institute (1988) as part of the NORSAR study (1988). Soil column characteristics were based on results from soil exploration - soil boring - laboratory testing performed at North Sea platform locations and onshore Norway locations. The earthquake response analyses were performed using the SHAKE computer program discussed earlier. The soil columns were organized into two different categories: Soil Type B - shallow firm alluvium, and Soil Type C - deep firm alluvium. Recorded earthquake time histories characteristic of those expected for the Norwegian seismotectonic conditions were used as input to the soil column analyses.

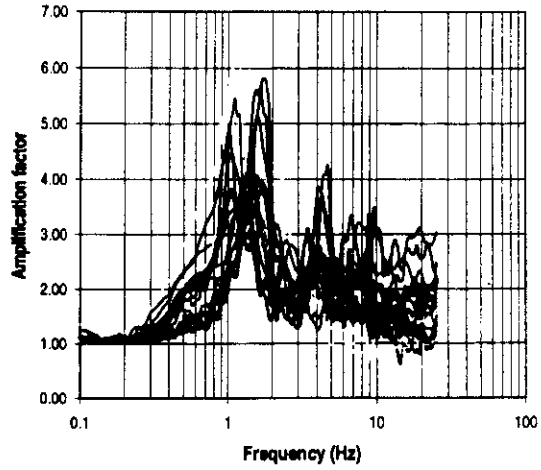

Figure 3.4: Computed Earthquake Response Spectra Amplification Factors for Deep Alluvium Soil Conditions (Soil Type C)

The amplification factors for the Soil Type B profiles has a definite peak in the period range of 0.05 sec to 0.1 sec. The peak amplifications range from about 2.5 to as high as 6. The very high amplifications in this long period range are apparently due to the low frequency content of the recorded earthquake ground motions used to perform the soil column response analyses.

The amplification factors for the Soil Type C profiles has a definite peak in the period range of 0.5 sec to 1 sec. The peak amplifications range from about 2.5 to almost 6.

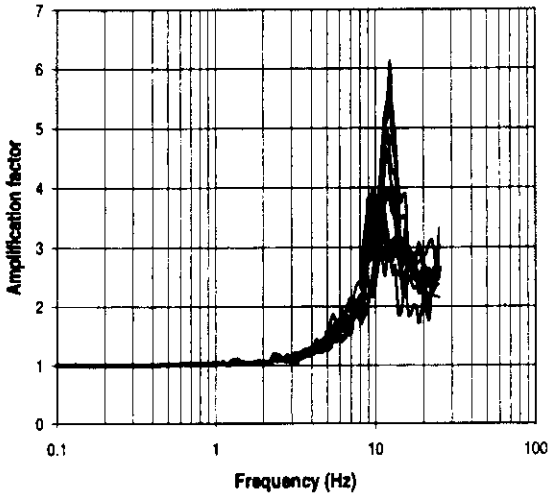

Figure 3.5: Computed Earthquake Response Spectra Amplification Factors for Shallow Alluvium Soil Conditions (Soil Type B)

Figure 3.6 summarizes the mean soil response spectra amplification factors for the two different soil column conditions. The mean peak soil amplification factor for Soil Type B is 3 and the same factor for Soil Type C is 3.5. These results confirm the need to have a factor that modifies the magnitude of the peak in the response spectra as a function of the soil conditions. The amplification factor for Soil Type C is comparable with that in the proposed ISO guidelines. The Soil Type B amplification factor also is comparable with that in the proposed ISO guidelines. However, the frequency content of the NORSAR Soil Type B spectrum is dramatically different from that in the proposed ISO guidelines.

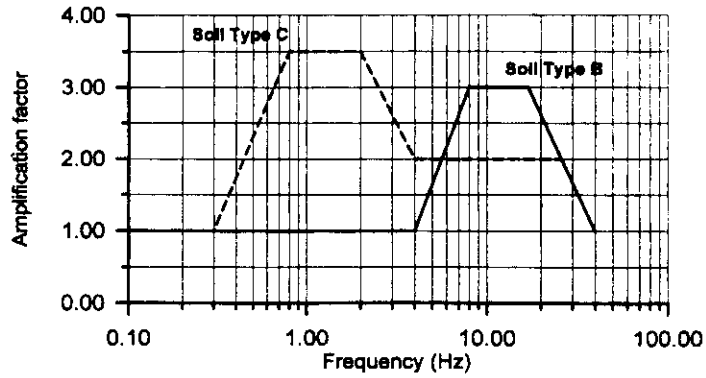

Figure 3.6: Recommended Earthquake Response Spectra Mean Amplification Factors for Soil

Figure 3.7 compares the ISO Soil Type B SLE spectra with that from the UK – Norwegian studies for Soil Types B and C.

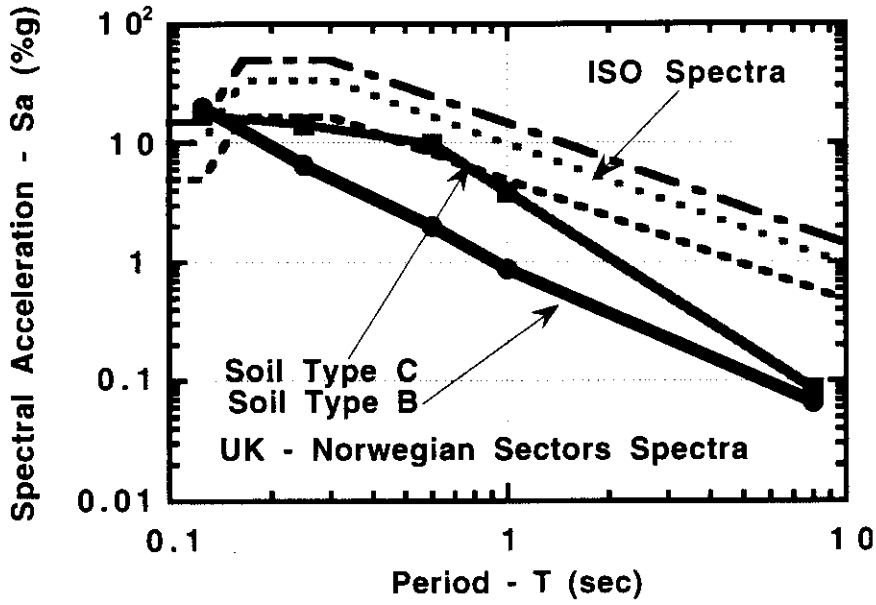

Figure 3.7: Comparison of Proposed ISO SLE Soil Spectra with the Soil Spectra from the UK – Norwegian Studies

This comparison indicates that the ISO spectra are somewhat more conservative than those from the UK and NORSAR studies. In the period range greater than about 1 second, the spectral accelerations of the proposed ISO spectra are about a factor of 10 greater than those indicated by the UK and NORSAR studies.

3.2 Gyda Platform North Sea Site Specific Spectra

The site – platform specific design spectra for the British Petroleum Gyda platform (Norwegian Block 2/1) are summarized in Figure 3.8 (Kvaerner Engineering A/S, 1988; Norwegian Geotechnical Institute and NTNF / NORSAR, 1987). Spectra for return periods of 100 years and 10,000 years for bedrock and the horizontal and vertical spectra at the sea floor are shown. The soils at the Gyda platform location are very firm alluvium consisting of interbedded dense sands and very stiff clays to a depth of 150 m.

Figure 3.9 compares the Gyda site specific criteria with that from the proposed ISO guidelines. The ISO guideline soil condition B

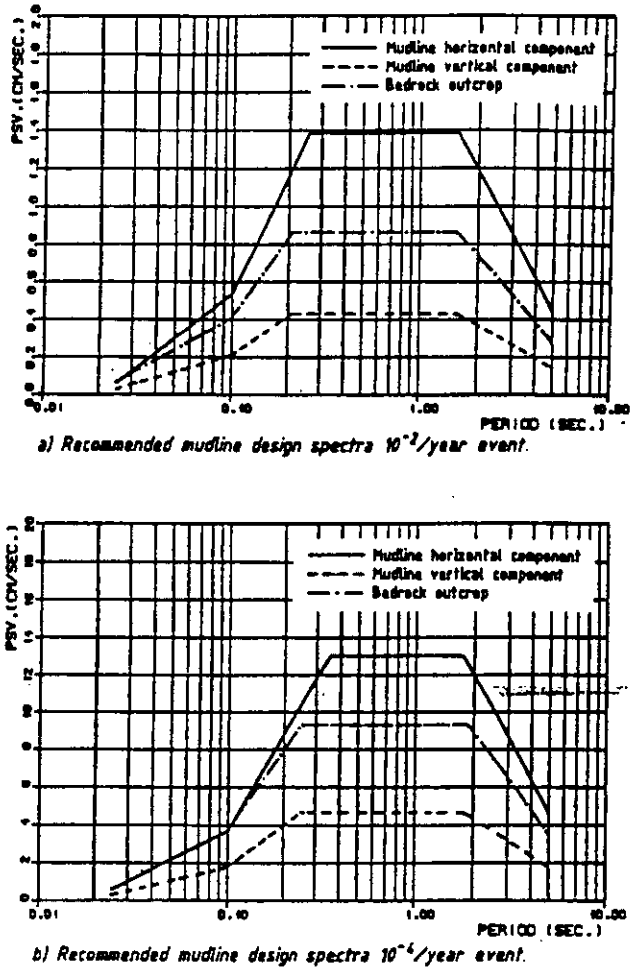

Figure 3.8: Gyda Platform Site Specific Spectra

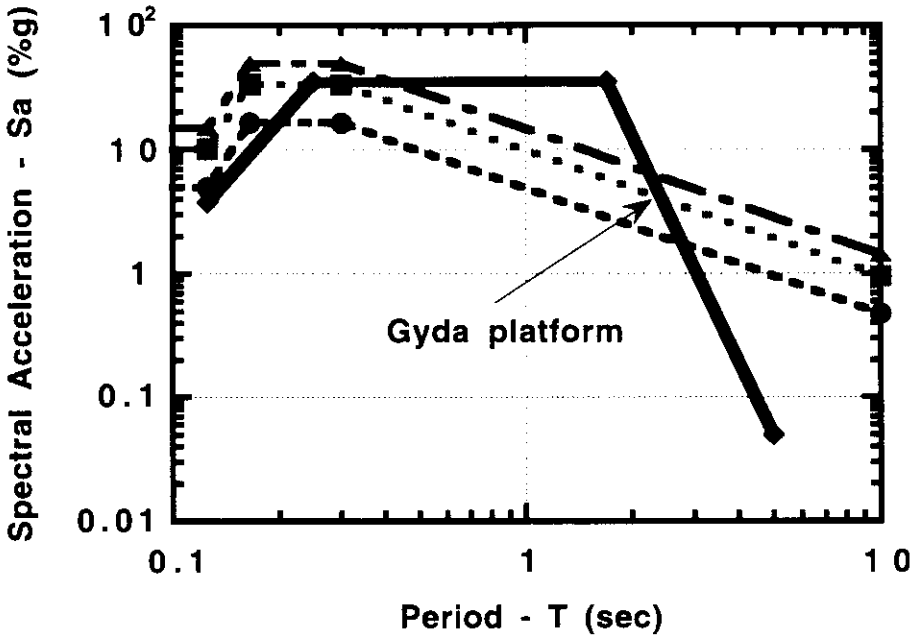

Figure 3.9: Comparison of Gyda Site specific SLE Spectra With Proposed ISO Guidelines SLE Spectra

is shown for the prescribed range in PGA. The Gyda platform has a fundamental period of T = 2.7 sec. The comparison at this period indicates that the ISO criteria would develop comparable forces on the platform. However, for periods, down to about 0.3 sec. the Gyda spectra would result in higher forces induced in the platform. The Gyda site specific spectra are very different from those derived in the UK (EQE International Ltd., 1998) and NORSAR (1998) studies.

3.3 Sierra Platform Offshore Indonesia Site Specific Spectra

The Unocal Sierra platform is located in the Makassar strait offshore Kalimantan, Indonesia. Figure 3.10 summarizes the 200 year return period SLE (a) spectra used to design this platform (Miller, 1993; Risk Engineering, 1992). The response spectrum indicated as (b) is the Ductility Level Earthquake (DLE). The dashed lines represent the API spectral shape. The soils at this location consist of deep, firm alluvium (interbedded clays and sands).

Figure 3.11 compares the site specific spectra with those derived from the proposed ISO guidelines for offshore Indonesia (Bea, 1998b). The Sierra platform has a fundamental period of about 2.1 seconds. In this range of periods, the ISO spectra provide an excellent fit to the site specific SLE spectra.

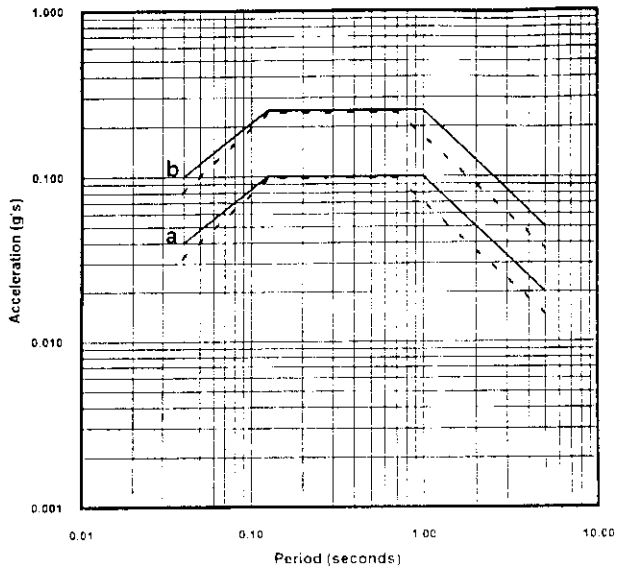

Figure 3.10: Sierra Platfor Site Specific SLE and DLE spectra

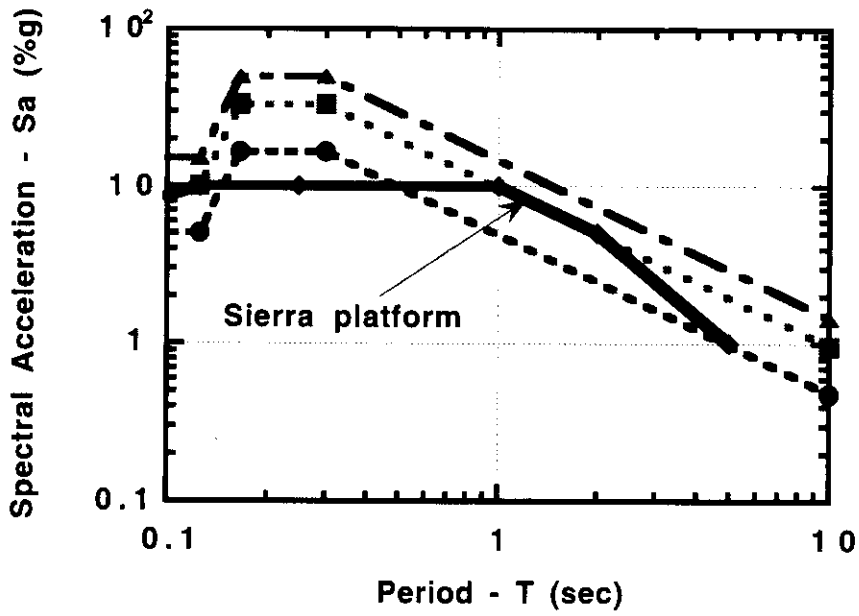

Figure 3.11: Comparison of Proposed ISO SLE and Sierra Platform SLE Spectra

3.4 Maui B New Zealand Site Specific Spectra

The Maui B platform is located between the North and South islands of New Zealand. Figure 3.12 shows the site specific SLE spectra developed for this platform location (Crouse, Quilter, 1991; Dolan, Crouse, Quilter, 1992). The design spectrum in this case was defined at a return period of 350 years. The soil conditions at this location consist of dense firm alluvium to a depth of 200 m.

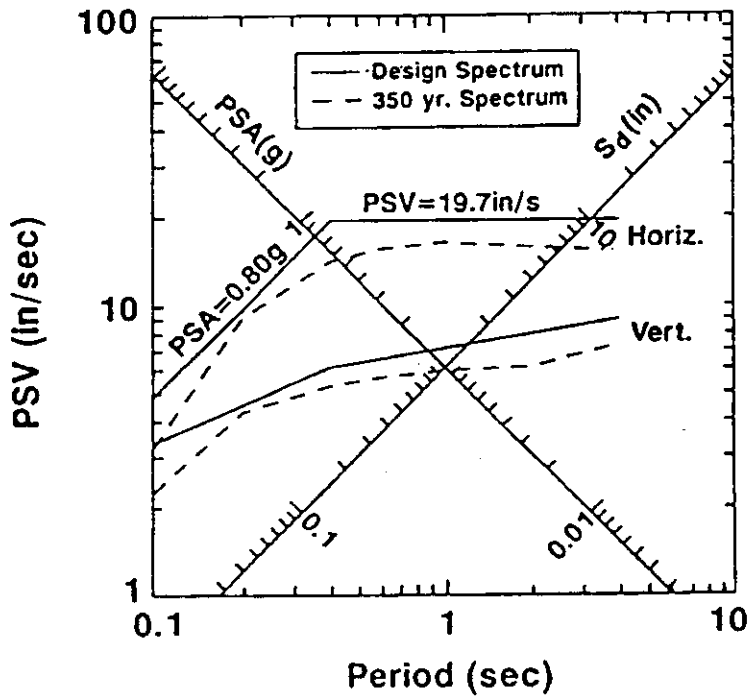

Figure 3.12: Maui B New Zealand 350 year Uniform Hazard Spectra and SLE Design Spectra

Figure 3.13 compares the proposed ISO 200 year SLE spectrum with the Maui B 350 year SLE spectrum. There is excellent agreement of both magnitudes and shapes of these two spectra. If the Maui B spectrum were adjusted to the same return period as the proposed ISO spectrum, the agreement would be even better.

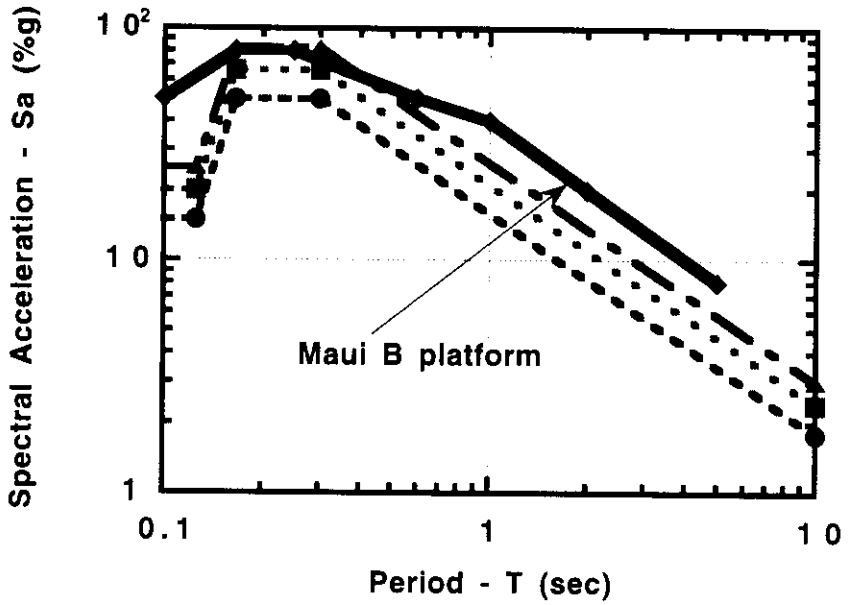

Figure 3.13 compares the Maui B site specific spectra for the defined 350 year SLE design event.

3.5 Summary

Benchmark studies of site specific spectra have been conducted to compare the proposed ISO spectra with those from site specific studies. In general, the proposed ISO spectra compare well with the region and site specific study results. The ISO spectra generally provide a conservative estimate of the response spectra ordinates in the range of natural periods of the offshore platforms. Given that the proposed ISO response spectra guidelines are consistent with those used to design the platforms at the locations studied, the comparisons indicate that the ISO guidelines should result in earthquake forces that are comparable and compatible with those derived from the site specific studies.

This page left blank intentionally

Chapter 4

Summary and Conclusions

4.0 Summary

The objective of this study was to continue development of earthquake load and resistance factor design (LRFD) guidelines with a benchmark study of earthquake loading results from site and platform specific studies. This study addressed two benchmark comparisons

a) comparison of the earthquake loadings induced in four platforms based on the proposed ISO guidelines and those from the current API (1993) guidelines; and

b) comparison of the SLE design response spectra for sites in the UK and Norwegian Sectors of the North Sea, offshore Indonesia, and New Zealand.

The comparisons indicate that the proposed ISO SLE spectra produce loadings on conventional template-type offshore platforms that are consistent with those based on current API SLE spectra guidelines. The proposed ISO SLE spectra are indicated to produce forces that are generally conservative when compared with those from recent UK and Norwegian Sector regional studies, but very close to the site-specific Gyda platform results. The proposed ISO SLE spectra are indicated to produce forces that are very close to those determined from the site specific studies offshore Indonesia and New Zealand.

4.1 Conclusions

The results from this study indicate that the proposed ISO SLE spectra guidelines generally provide conservative estimates of the loadings based on current API guidelines and regional and site specific studies in the UK and Norwegian Sectors of the North Sea, offshore Indonesia and New Zealand.

4.2 Acknowledgments

The author would like to acknowledge the assistance and information provided on the Gyda platform seismic studies by Mr. R. Snell, Mr. R. Corr, and Dr. Peter Gorf of BP Exploration, Middlesex, UK.

This page left blank intentionally

References

American Petroleum Institute (API) (1993). *Recommended Practice for Planning, Designing and Constructing Fixed Offshore Platforms – Load and Resistance Factor Design*, API Recommended Practice 2A-LRFD, American Petroleum Institute, Washington, DC

Bea, R. G. (1996). "Probability Based Earthquake Load and Resistance Factor Design Criteria for Offshore Platforms," *Proceedings Offshore Technology Conference*, OtC 8106, Society of Petroleum Engineers, Richardson, TX.

Bea, R. G. (1997a). "Background for the Proposed International Standards Organization Reliability Based Seismic Design Guidelines for Offshore Platforms," *Proceedings of the Earthquake Criteria Workshop: Recent Developments in Seismic Hazard and Risk Assessment*, 16th International Conference on Offshore Mechanics and Arctic Engineering, Yokahama, Japan, (obtain proceedings from Port and Harbors Research Institute, Yokuska, Japan).\

Bea, R. G. (1997b). *Risk Based Oceanographic and Earthquake Load & Resistance Factor Criteria for Design and Requalification of Platforms Offshore Indonesia*, Report to Indonesian Petroleum Association, Directorate General of Oil and Gas of Indonesia, Pertamina, and Bandung Institute of Technology, Marine Technology and Management Group, University of California at Berkeley.

Bea, R. G. (1998a). *Continued Development of Earthquake Load and Resistance Factor Design Guidelines, Report 1 - Concrete Gravity Base Structures LRFD Guidelines*, Report to the UK Health and Safety Executive, Marine Technology and Management Group, University of California at Berkeley.

Bea, R. G. (1998b). *Continued Development of Earthquake Load and Resistance Factor Design Guidelines, Report 2 – Seismic Hazard Characterizations*, Report to the UK Health and Safety Executive, Marine Technology and Management Group, University of California at Berkeley.

Crouse, C.B., and Quilter, J., (1991). "Seismic Hazard Analyses and Development of Design Spectra for Maui A Platform," *Proceedings of the Pacific Conference on Earthquake Engineering*, Auckland, New Zealand.

Dolan, D. K., Crouse, C. B., and Quilter, J. M. (1992). "Seismic Reassessment of Maui A," *Proceedings of the Offshore Technology Conference*, OTC 6934, Society of Petroleum Engineers, Richardson, Texas.

EQE International Ltd. (1998). *Seismic Hazard Mapping of Offshore Britain*, Report to Health and Safety Executive, London, UK.

Kvaerner Engineering A/S (1988). *Gyda Project Dossier Design Documentation, Jacket Structure*, Report to BP Petroleum Development (Norway) Limited, UA.

Miller, T. M. (1993). *Seismic Analysis of Indonesia's Sierra Wellhead Platform*, Unocal Energy Resources Technology Division, Production & Development Technology Department, Project Report No. 93-26, Unocal Corporation, Brea CA.

NORSAR and Norwegian Geotechnical Institute (1998). *Seismic Zonation for Norway*, Report to Norwegian Council for Building Standardization.

Norwegian Geotechnical Institute and NTNF / NORSAR (1987). *Gyda Field Development Project Earthquake Loading Criteria Assessment*, Report to BP Petroleum Development (Norway) Limited U/A, Oslo, Norway.

Norwegian Geotechnical Institute (1998). *Effects of Local Soil Response on Earthquake Loading*, Report to Norwegian Council for Building Standardization.

Risk Engineering, Inc., 1992, *Seismic Hazard Analysis for the Offshore Kalimantan Sites Indonesia*, Report to Unocal Corporation, March 27.

Stear, J. D., and Bea, R. G. (1998a). *TOPCAT – Template Offshore Platform Capacity Assessment Tools*, Report to Joint Industry Sponsors, Marine Technology & Management Group, University of California at Berkeley.

Stear, J. D., and Bea, R. G. (1998b). "Simplified Strength-Level Earthquake Assessment of Jacket-Type Platforms," Proceedings 8th International Conference on Offshore and Polar Engineering, Society of Offshore and Polar Engineers, Golden, CO.

Stear, J. D., and Bea, R. G. (1999). *A Static Assessment Approach for Jacket-Type Platforms in Seismically Active Regions*, Report to Screening Methodologies Project Phase IV Joint Industry Project Sponsors, Marine Technology & Management Group, University of California at Berkeley.

Appendix A

Simplified Strength Level Earthquake Assessments of Jacket Type Platforms

A.1 Introduction

This Appendix summarizes a simplified method with which strength-level earthquake analyses of jacket-type platforms can be performed. By examining the primary bending, shear, and foundation rotation responses, estimates of platform vibration characteristics can be obtained from which earthquake forces can be estimated by the response spectrum method. This process is referred to as SRSA (Simplified Response Spectrum Analysis). These forces can then be taken together with capacities derived from ULSLEA (Ultimate Limit State Limit Equilibrium Analysis) to develop an evaluation of the demand-capacity behavior of the platform. The ULSLEA-SRSA method is applied to the assessment of two platforms. Results from 3-D frame analyses of the two platforms are used for validation of the simple approach. Agreement between the ULSLEA-SRSA and detailed 3-D analyses is excellent.

Several studies related to the simplified assessment of platforms subject to earthquakes are documented in this paper. In the first, a design code approach to earthquake forces based on that contained with the Uniform Building Code is demonstrated and compared to more detailed earthquake force estimates. Next, common simple approximations to pile-head stiffnesses are reviewed, and the impact of foundation flexibility on platform response examined. Last, the impact of local inertia forces on brace axial capacity is studied.

During the past five years there has been growing interest in the development of simplified structural analysis methods which are inexpensive to apply yet provide sufficiently accurate results to help make timely and economic engineering assessments. A major reason for this development is the re-assessment of aging infrastructure. As many structures (buildings, bridges, offshore platforms, etc.) approach the end of their original service lives, many owner/operators desire to keep these structures in service. As many of the structures in existence today were designed for much less stringent load criteria than current code recommendations, some form of analysis must be performed.

While there are many structural analysis tools available today to perform detailed assessments, these tools usually require a high degree of expertise to operate, and to apply to a large number of structures would be prohibitive in terms of time and money. What is needed is a staged process of assessment, by which the bulk of the structure population can be assessed quickly using cheap, conservative methods, leaving the more problematic cases for further rigorous analysis.

Previous work has been performed by the Marine Technology and Management Group at U. C. Berkeley concerning the development and verification of simplified analysis methods for offshore

platforms. This earlier effort addressed the evaluation of jacket-type platforms subject to wind and wave forces, and resulted in the procedure known as ULSLEA (Ultimate Limit State Limit Equilibrium Analysis). Based on a simple demand-capacity format, and considering only the primary failure mechanisms in a platform (hinging of unbraced deck legs, diagonal brace buckling in the jacket bays, exceeding of pile group lateral or overturning capacity), procedures were developed to estimate loads and platform component capacities (Bea, Mortazavi, 1995). This demand-capacity procedure has been the subject of much testing and verification; readers are referred to Bea, et al. 1995; Mortazavi and Bea, 1997; and Stear and Bea, 1997.

This Appendix documents a simplified procedure for estimating earthquake forces which is intended to compliment ULSLEA-based capacity procedures. Using simplified estimates of the primary bending, shear and foundation responses of the platform, vibration properties for the platform are approximated. Then, through application of response spectrum analysis, earthquake demands on the platform are estimated. This process is referred to as SRSA: Simplified Response Spectrum Analysis. It is intended to allow for the estimation of earthquake forces without resorting to detailed finite-element models.

The ULSLEA-SRSA approach is used to assess two platforms: a 4-leg and an 8-leg. To verify the accuracy of the ULSLEA-SRSA approach, 3-D frame analyses of these platforms has been performed, and the results from these more detailed analyses compared to those from ULSLEA-SRSA. The results are found to be in excellent agreement; application of ULSLEA-SRSA yields earthquake failure intensities (the zero-period acceleration for the API RP 2A response spectrum [API, 1993] associated with the load at first member failure) within 15 % of those found from the 3-D frame analyses.

In addition to describing the ULSLEA-SRSA method and demonstrating its application, three other studies related to simple assessment of jacket-type platforms subject to earthquakes are also documented in this paper. The first study demonstrates an alternative method to estimating earthquake forces based on a modified Uniform Building Code approach (UBC, 1994). The second reviews several common approximations to pile-head stiffnesses, and demonstrates the sensitivity of platforms to foundation flexibility. Finally, the significance of local forces on tubular braces is investigated.

A.2 Estimating Seismic Demands: SRSA

The procedure by which seismic demands are estimated for the platform components (deck bay, jacket bays, and foundation) is based on response spectrum analysis; it is referred to as SRSA: Simplified Response Spectrum Analysis. By considering the primary bending, shear and foundation displacement mechanisms in the platform, simple estimates of platform vibration properties are made. These properties are then used together with response spectrum analysis to develop appropriate earthquake loads on the platform.

Response Components

The horizontal response of a platform can be thought of as consisting of three components (Figure 1):

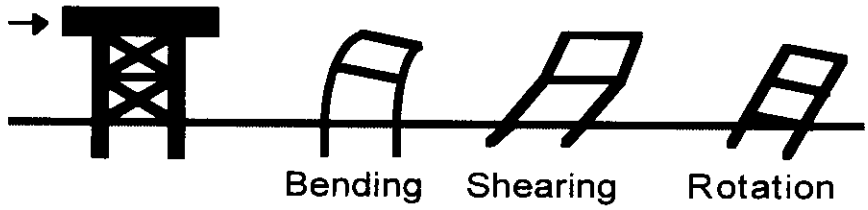

Figure 1: Horizontal Response Components

There is a bending component, from the cantilever deflection of the platform due to the axial loads on the piles from overturning; a shear component, from the shear deformations of each braced jacket bay and the foundation, and a rotation component due to tension and compression of the piles.

Using very simple structural relationships, it is possible to establish the load-deflection properties of each individual response component without much effort. Deflections due to bending can be found from:

$$\Delta = \frac{PL^3}{3EI} \tag{1}$$

where I refers to the moment of inertia of the platform tower structure based on the platform pile cross sections. Shear deflections can be found by considering the deformation of the individual shear mechanisms at each level in the platform. For a braced jacket bay, the shear stiffness is:

$$k_{bay} = \Sigma k_i \cos^2 \vartheta_i \tag{2}$$

where:

k_i = axial stiffness of each individual brace, i.e. EA/L
θ_i = angle between each brace and the horizontal

For bays which do not have braces (the deck bay on many platforms do not) the shear deformation will be controlled by the bending of the platform legs. In this case, the shear stiffness is:

$$k_{bay} = \Sigma k_i \tag{3}$$

where:

k_i = effective horizontal stiffness of each individual leg assuming fixed-fixed conditions, i.e. $12EI/L^3$

The shear stiffness at the foundation level will be the sum of the pile-head lateral stiffnesses.

Deflections from foundation rotation can be calculated by considering the platform to be a rigid structure mounted on a rotational spring. This spring is the sum of the products of the axial stiffnesses of the piles and the square of their distance from the platform axis of rotation (either end-on or broadside).

Considering the platform to be a system of lumped masses (one at each horizontal framing level, the decks, and the mudline), the flexibility matrix for this simple system can easily be constructed by summing the component responses to unit loads at each level. The vibration properties of the system can then be found through solution of the standard eigenvalue problem of the form:

$$\mathbf{fm}\phi_n = \frac{1}{\omega_n^2}\phi_n \tag{4}$$

where:

$\mathbf{f}$ = matrix of flexibility coefficients
$\mathbf{m}$ = matrix of lumped masses
ϕ = mode shape
ω = natural frequency

This form has the advantage of converging to the largest values of $1/\omega^2$ with each iteration, which correspond to the largest periods. In this fashion, the first mode will be found first, then the second, and so on.

If modal analysis is not possible, this approach conveniently provides displacements which can then be used together with Rayleigh's method to obtain approximate vibration periods:

$$T_1 = 2\pi\sqrt{\frac{\sum_{j=1}^{N} m_j u_j^2}{g\sum_{j=1}^{N} m_j u_j}} \tag{5}$$

$$\phi_1 = \mathbf{u} / u_{\max} \tag{6}$$

where $\mathbf{u}$ is the vector of nodal displacements associated with nodal forces gm_j. This approach is very amenable to hand calculation.

Masses are concentrated at each horizontal framing level and at the deck. These masses include the mass of any hydrodynamic added mass or contained mass, marine growth, mounted equipment, and conductors. For cylindrical members, the approximate hydrodynamic added mass per unit length is defined by (Clough, 1960):

$$m_{added} = K\rho_w \pi r^2 \sin\theta \tag{7}$$

where:

K = flexibility factor for members; ranges from 0.6 for pinned-end members to 1.0 for fixed-end members
ρ_w = density of the surrounding fluid
r = radius of the member
θ = the angle between the cylindrical length axis and the direction of translation

To account for proximity to the free surface, the added mass is further scaled according to (Goyal, Chopra, 1989):

$$m_{added}(z) = m_{added} \text{ when } z > 0.1\ H_o \tag{8}$$

$$m_{added}(z) = m_{added}(z / 0.1\ H_o) \text{ when } z \leq 0.1\ H_o \tag{9}$$

where:

z = depth below the surface
H_o = water depth

Soil mass consisting of the soil contained within the piles to a depth of five pile diameters is included in the mass lumped at the mudline.

Platform vertical response can be determined in a similar fashion. In this case, only the axial stiffnesses of the jacket legs and piles are used to construct the flexibility matrix; the solution procedure to find vertical modes will be the same as for horizontal modes.

For platforms possessing significant mass and/or stiffness eccentricities, torsion response can also be developed in a simple fashion. Rotational stiffnesses between framing levels can be developed based on the layout of the diagonal braces (or piles, for the foundation level), while mass moments of inertia can be derived from the spatial distribution of the mass as each level.

Modal Analysis and Demands

Together with an appropriate response spectrum, modal demands can be estimated as shown below for shear and overturning moment:

$$V_{in} = \sum_{j=1}^{N} \Gamma_n m_j \varphi_{jn} \left(\frac{4\pi}{T_n^2} \right) D_n \text{, shear for } i^{th} \text{ level} \tag{10}$$

$$M_{bn} = \Gamma_n L_n^{\theta} \left(\frac{4\pi}{T_n^2} \right) D_n \text{, overturning moment} \tag{11}$$

where:

D_n = modal displacement from response spectrum
n = mode index
j = DOF index

The individual modal responses can then be combined to find the total response on a given component. The square-root sum-of-the-squares (SRSS) rule is commonly used within civil engineering practice; however, as noted in API RP-2A, this rule can on occasion provide results which are unconservative when compared to a time-history analysis.

A.3 Platform Component Capacities: ULSLEA

The strength limits for platform components are determined through application of ULSLEA (Mortazavi, 1995). The strength formulations for these components are listed in the following sections.

Unbraced Leg Sections

The ultimate shear force which can be resisted by an unbraced section in the platform structure is based on bending capacities of the tubular legs in the section. Assuming the formation of a story mechanism based on the simultaneous hinging of the legs at the top and bottom of the structural bay, and accounting for P-Δ effects, the shear capacity of the bay can be estimated from:

$$P_u = \frac{2nM_u}{H_d} - V_{P\Delta} \tag{12}$$

where:

$$V_{P\Delta} = \frac{QD}{H_d}, \text{ P-}\Delta \text{ effects due to drift or displacement } D \tag{13}$$

$$M_u = M_{cr} \cos\left(\frac{\pi Q / n}{2P_{cr}}\right), \text{ ultimate leg moment} \tag{14}$$

and:

H_d = height of bay
M_{cr} = critical moment, governed by local buckling
Q = vertical force on bay
P_{cr} = critical axial load, governed by local buckling
n = number of legs

Braced Bays

The shear force which can be resisted by a braced bay is dependent on the axial tension and compression capacities of the bracing members and their connections to the legs. A mechanism is assumed to form when the first member in the load path fails; i.e. the bay is assumed to possess no strength beyond first yield.

Based on a three-hinge failure mode, the exact solution for the bending moment in a beam-column at collapse is:

$$M_u = \left(\frac{1}{1 + 2\frac{\sin 0.5\varepsilon}{\sin\varepsilon}} \right) \frac{1}{\varepsilon^2} \left(\frac{1}{\cos 0.5\varepsilon} - 1 \right) \left(wl^2 + 8 P_u \Delta_0 \right) \tag{15}$$

where:

$$\varepsilon = l\sqrt{\frac{P_u}{EI}} \tag{16}$$

and:

P_u = ultimate axial capacity
w = distributed local load
l = length of brace
Δ_0 = initial out-of-straightness
E = elastic modulus
I = cross-section moment of inertia of brace

Using P-M interaction in the brace as a second equation relating M_u and P_u:

$$\frac{M_u}{M_p} - \cos\left(\frac{\pi P_u}{2 P_p} \right) = 0 \tag{17}$$

where:

M_p = plastic moment capacity of brace cross section
P_p = tension capacity of brace cross section

Solving for Δ_0 assuming $P_u = P_{cr}$ from API RP 2A (1993), it is possible to solve for P_u using iteration.

The distributed local load w on the brace is assumed to result from local response of the brace to earthquake excitation. To estimate the local acceleration on the brace, it is possible to treat the brace as mounted equipment, and then apply a procedure such as that described by Bowen and Bea (1995) to determine the filtered response.

Tubular joint tension and compression capacities can be established through application of empirical formulas documented in API (1993). It should be noted that these equations are somewhat conservative.

Overall bay capacity will be given by:

$$P_{u_{bay}} = \sum_{i=1}^{N} D_{1st} K_i + F_{1L} \tag{18}$$

where:

D_{1st} = failure displacement of most likely member to fail, found from the smallest ratio of P_u/K
K = effective horizontal stiffness of individual braces
P_u = minimum of brace strength or connections to which brace is attached
F_{1L} = batter forces from legs

No reduction is taken for local P-Δ effects, as these are generally quite small for braced sections due to the smaller displacements needed to mobilize horizontal capacity.

It should be noticed that if there is an unbraced portal above a braced section, there could be noticeable reduction in the capacity of the braced section due to the need to balance the large bending moments in the legs of the unbraced section (Mortazavi, 1995). This can be accounted for by further reducing the shear capacity of the braced section by the effective shear needed to balance the leg moments.

Pile Horizontal Capacity

The horizontal capacity of the foundation is determined in a manner similar to that for an unbraced leg section, with the exception that the horizontal support provided by the surrounding soils and the batter shear component of the piles are included.

For a pile deeply imbedded in cohesive soils, the ultimate horizontal force that can be resisted at the pile top is given by (Tang, Gilbert, 1990):

$$P_u = 0.5\left\{-\left(2.7D^2 S_u + 1.8 S_u XD\right) + \sqrt{\left(2.7D^2 S_u + 1.8 S_u XD\right)^2 + 14.4 S_u D M_p}\right\} \tag{19}$$

where:

M_p = plastic moment capacity of a pile
D = pile diameter
S_u = effective undrained shear strength of the soil
X = scour depth

For cohesionless soils, the pile capacity is given by (Tang, Gilbert, 1990):

$$P_u = 2 M_p \left(X + 0.544 P / \left(\gamma D \tan\left(45 + \phi / 2\right)\right)\right) \tag{20}$$

where:

ϕ = effective angle of internal friction of the soil

γ = submerged unit weight of the soil

Pile Axial Capacity

The axial yield capacity of a pile is based on the combined effects of a shear yield force acting on the surface of the pile and a normal yield force acting over the pile end. Capacity is thus given by:

$$Q = qA_p + f_{av}A_s \tag{21}$$

where:

q = normal end yield force per unit of pile-end area
f_{av} = average shear yield force per unit of embedded shaft surface area
A_p = area of pile tip
A_s = embedded shaft surface area

Approximations for q and f_{av} for cohesive and cohensionless soils can be found in Mortazavi (1995).

A.4 Application of ULSLEA – SRSA

To assess the accuracy of the ULSLEA-SRSA approach relative to more rigorous analysis, the simple method was used to determine the demand-capacity behavior of two platforms: a 4-leg and an 8-leg. From the demand-capacity profiles established for each platform, the earthquake intensity (expressed as the response spectrum zero-period acceleration or ZPA) necessary to generate loads resulting in the formation of a collapse mechanism were calculated. These collapse intensities were then compared to collapse intensities calculated from 3-D response spectrum analyses of each platform using a 3-D frame model. The following sections describe each platform, and the results obtained from analyzing them using both the simple approach and the 3-D analysis.

Platform A

Platform A is a hypothetical design for a symmetric 4-leg production platform (see Figure 2). The structure is designed for 100 ft water depth. The deck is at +50 ft MWL and supports a load of 5,000 kips. The main diagonals in the first jacket bay are 24 in.-diameter (w.t. 0.5 in.), while those in the second bay are 30 in.-diameter (w.t. 0.625 in.); the diagonals in the deck bay are 36 in.-diameter (w.t. 0.75 in.). The legs are 78 in.-diameter (w.t. 0.875 to 1.125 in.); they are grouted, and possess heavy joint cans. The piles are 72 in.-diameter (w.t. 1 to 1.5 in.), and are designed for 150 ft penetration in medium to stiff clay. The shear strength of the clay is 2.5 kips/ft^2 at the surface, and increases by 0.01 kip/ft^2 per ft of depth. The pile ends are founded on a very stiff soil layer (rock) which has a shear strength of 184 kips/ft^2. All steel is A36.

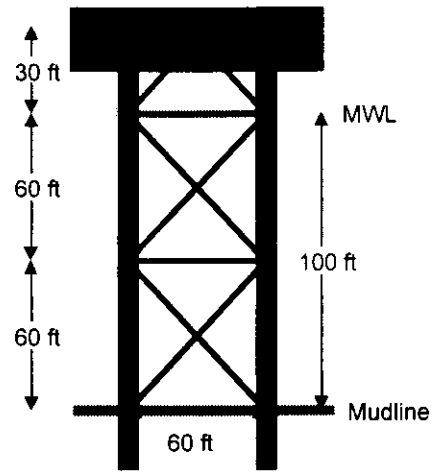

Figure 2: Platform A

The platform was analyzed using both ULSLEA-SRSA as well as 3-D response spectrum analysis. For the 3-D response spectrum analysis, joints were assumed to be rigid, and the deck was assumed to act as a rigid diaphragm. Tubular steel member axial strengths were taken from buckling strength curves (API, 1993). Imbedded pile performance was established by modeling a single pile as a segmented beam supported by springs (following the guidelines of API RP 2A, API, 1993), and then performing a series of analyses to determine pile-head force-displacement relationships suitable for use with a 3-D elastic model. The pile-head stiffnesses derived from these analyses were used in both the simple and 3-D analyses. For both the simple analysis and the 3-D analysis, the brace buckling length factor was taken to be 0.65, and a local acceleration of 1.0 g was applied to all members in the jacket to represent the local response contribution. Selected member properties are shown below in Tables 1, 2 and 3. It can be seen that the brace buckling strengths determined from limit equilibrium (ULSLEA) are slightly overestimated (by at most 8%) relative to those determined from empirical data, while the pile capacities are underestimated (in the range of 8 to 18%).

Each approach utilized the API Soil B response spectrum (API, 1993) to derive earthquake loads once vibration properties were established. Loads were assumed to act on all three platform principal axes; the square-root sum-of-the-squares (SRSS) rule was used to combine the individual modal and directional responses. The load case used in both analyses consisted of the load on one horizontal axis found using the API spectrum for a given ZPA combined with load on the other axis found using 67% of this ZPA and load on the vertical axis found using 50% of this ZPA. No torsional response was considered.

The major vibration characteristics of the structure estimated using the two approaches are shown below in Figure 3 and Figure 4. The simple method provides excellent estimates of the first two horizontal mode periods as compared with the 3-D frame analysis, but subsequent period estimates begin to deviate. The vertical mode period found from the simple method is also in good agreement with the period estimated in the 3-D frame analysis.

Table 1: Tubular Brace Capacities

Brace Diameter and Thickness	Axial Capacity (kips) - API	Axial Capacity (kips) - ULSLEA
24" ϕ 0.5"	1100	1190
30" ϕ 0.625"	1880	1920
36" ϕ 0.75"	2820	2890

Table 2: Pile Strengths

Pile Strength	Capacity (kips) - API	Capacity (kips) - ULSLEA
Tension	6000	4892
Compression	11200	10400
Lateral	1960	1750

Table 3: Pile Stiffnesses

Pilehead Springs	Stiffness
Vertical	3150 kips / in
Horizontal	470 kips / in
Rotational	40 x 10^6 kip-ft / rad

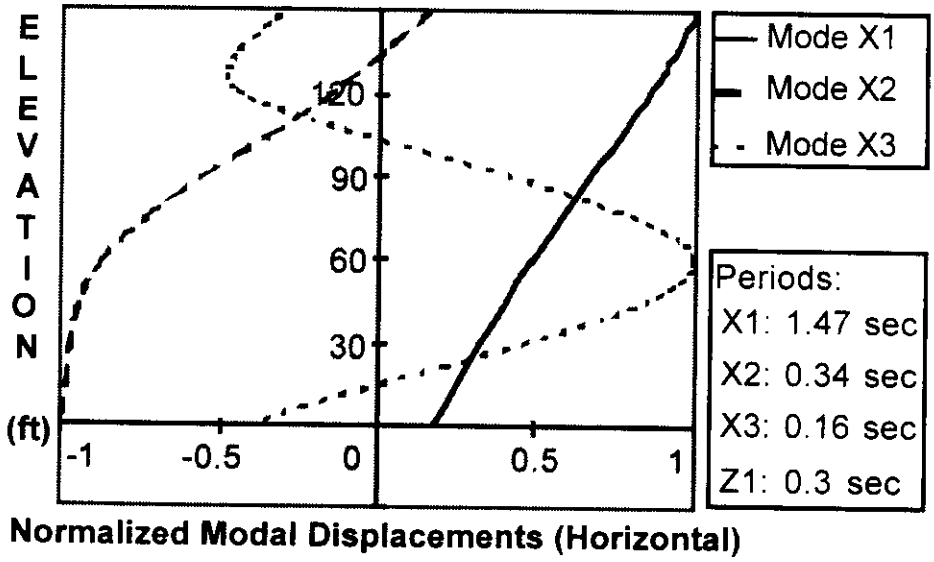

Figure 3: Platform Vibration Properties (3-D)

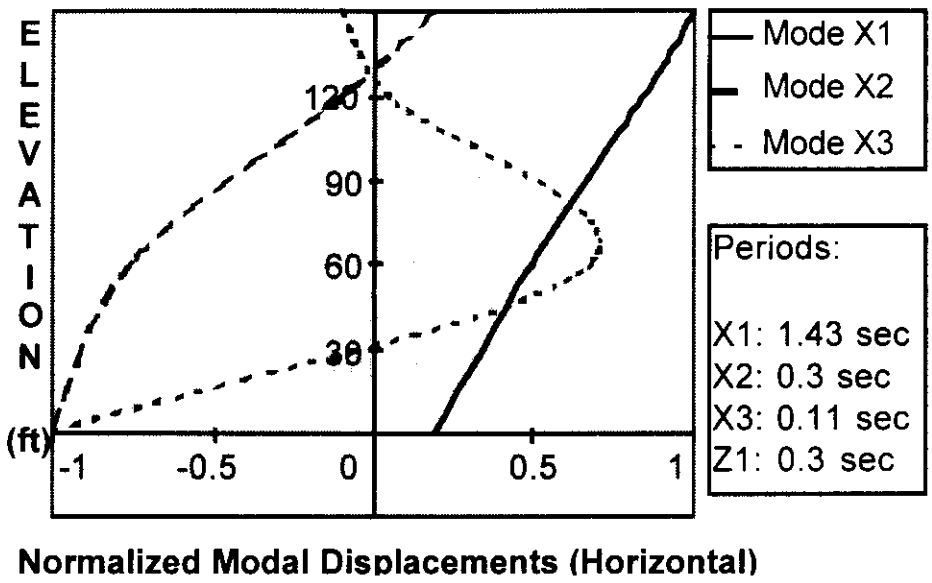

Figure 4: Platform Vibration Properties (SRSA)

Loads calculated from the two methods are, not surprisingly, in excellent agreement, given the agreement between the estimated platform vibration properties and the fact that most of the platform response is in the first few modes. Horizontal shears acting at each level along with peak pile loads are shown in Figure 5 and Table 4 for a spectrum ZPA of 0.25 g. The peak loads differ by at most 5%.

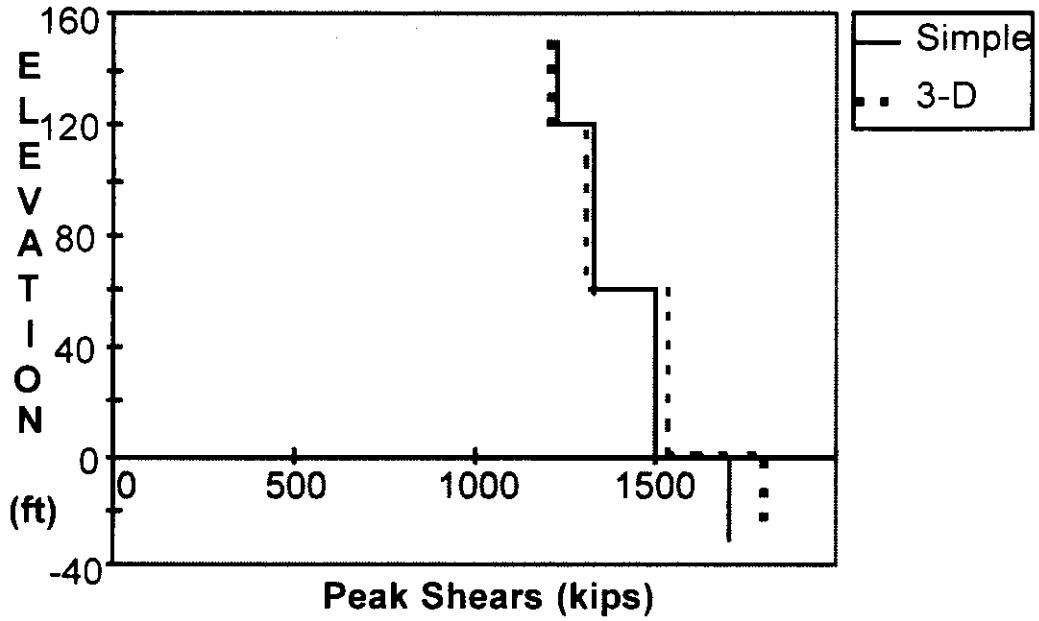

Figure 5: Platform Loads, ZPA = 0.25 g

Table 4: Pile Loads, ZPA = 0.25g

Pile Load	3-D (kips)	SRSA (kips)
Tension	359	362
Compression	3859	3862
Lateral	541	511

Using the simple method, the earthquake intensity resulting in the formation of a collapse mechanism is 0.625 g. Loads for this case and the associated platform capacity profile are shown in Figure 6. Failure is initiated by the buckling of the diagonal braces in the first jacket bay. The 3-D analysis indicates the earthquake intensity resulting in the formation of a collapse mechanism is 0.645 g (4% higher); this analysis also indicates the first elements to fail will be the diagonal braces in the first jacket bay. For this example application, ULSLEA-SRSA provides an excellent estimate of the earthquake intensity needed to cause the formation of a collapse mechanism, as compared to the results of the 3-D frame analysis.

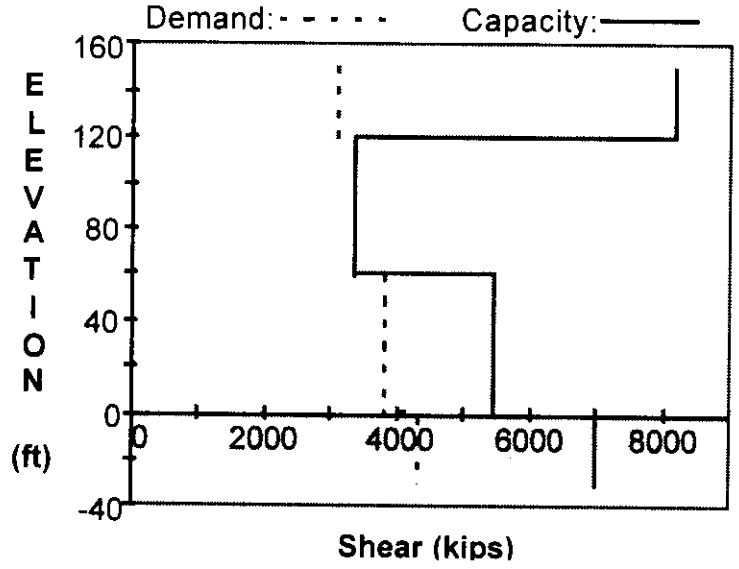

Figure 6: Demand - Capacity Shear Profile from ULSLEA-SRSA

Platform B: 8-Leg Structure

Platform B is an 8-leg drilling platform sited in 265 ft of water in San Pedro Bay off Southern California (see Figure 7). It was designed to support 80 24 in.-diameter conductors. The platform has two decks located at +45 ft MWL and +64 ft MWL respectively; the deck bay is braced. The jacket is battered 1:7 in the broadside direction, and 1:12 in the end-on direction. The main diagonals range from 20 in.-diameter (w.t. 0.75 in.) to 36 in.-diameter (w.t. 1.125 in.). The corner legs of the jacket are 71 in.-diameter (w.t. 1 in. to 2 in.), while the interior legs are 54 in.-diameter (w.t. 0.675 to 2 in.); the legs have heavy joint cans but are not grouted. The corner piles of the platform are 66 in.-diameter, and penetrate to 264 ft. The center piles are 48 in.-diameter, and penetrate to 232 ft. The soil at the site is predominantly clay (medium-stiff to stiff). The majority of the structural members are 36 ksi steel, while the piles are 50 ksi steel.

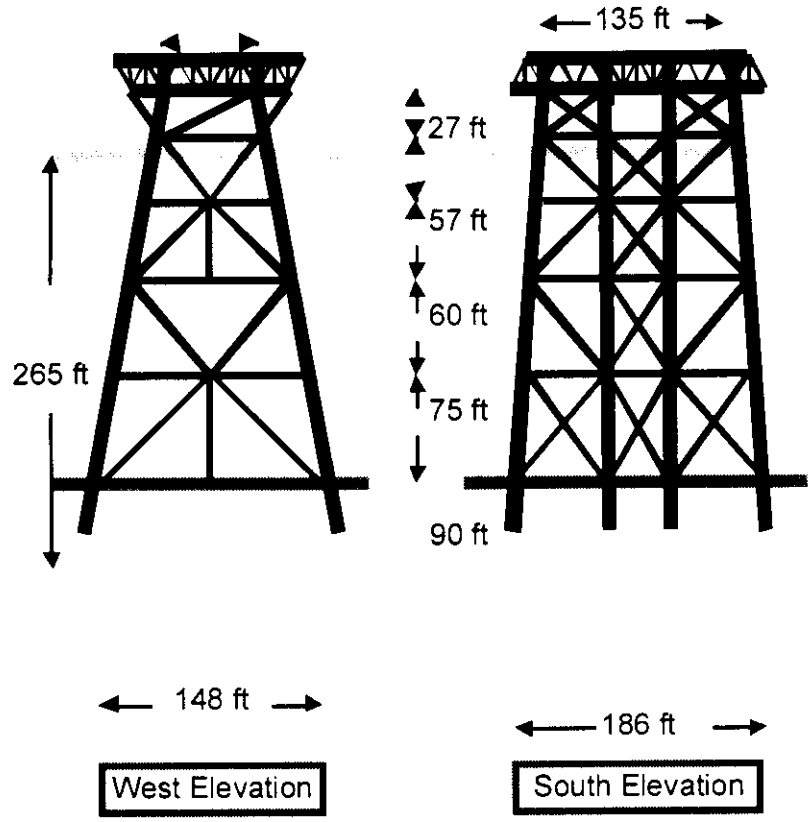

Figure 7: Platform B Elevations

This platform was also analyzed using both ULSLEA-SRSA as well as 3-D response spectrum analysis with a 3-D frame model. The same approaches taken for determining member strength and pile characteristics for Platform A were used in these studies. Joints were assumed to be rigid, and the deck was modeled as a rigid diaphragm. For both the simple and 3-D analyses, the brace buckling length factor was taken to be 0.65, and a local acceleration of 1.0 g was applied to all members in the jacket.

Each analysis utilized the API Soil B response spectrum (API, 1993) to derive earthquake loads once vibration properties were established. Loads were assumed to act on all three platform principal axes; the SRSS rule was used to combine the individual modal responses and directional responses. The platform was analyzed for two load cases: end-on and broadside. For each load case, the load on the major horizontal considered was combined with 67% of the load on the other horizontal axis, along with 50% of the load on the vertical axis. As the platform possessed no mass or stiffness eccentricities, no torsional response was considered.

The major vibration characteristics of the platform estimated using the two approaches are shown in Figure 8 to Figure 11. It should be noted that the simple method provides fundamental horizontal period estimates smaller than those from the 3-D frame analysis, especially for the end-on direction; this is due to the fact that the jacket is substantially more flexible in shear due to the absence of grouting. This additional shear or warping flexibility is not captured by the simple approach. When both the 3-D frame model and the simple model were changed to reflect grouting, the fundamental

horizontal periods for the end-on case became 2.24 sec (3-D) and 2.3 (SRSA), while the fundamental period estimates for the broadside case became 2.1 (3-D) and 2.2 (SRSA).

Loads calculated using the two methods for the original (un-grouted) case are still in very good agreement, with the simple loads being with 12 % of those from the 3-D frame. Horizontal shears acting at each level along with peak pile loads are shown in Tables 5 and 6 and Figure 13 and Figure 14 for a spectrum ZPA of 0.25 g. The platform's 80 conductors carry a substantial amount of the lateral load at the foundation level; this drives down the lateral load carried by the main piles.

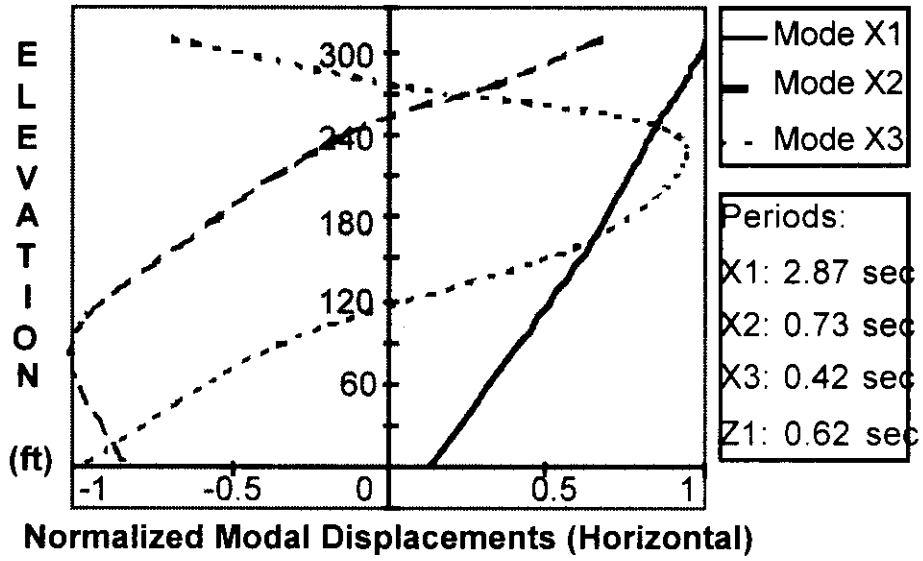

Figure 8: Platform Vibration Properties, End-On (3-D)

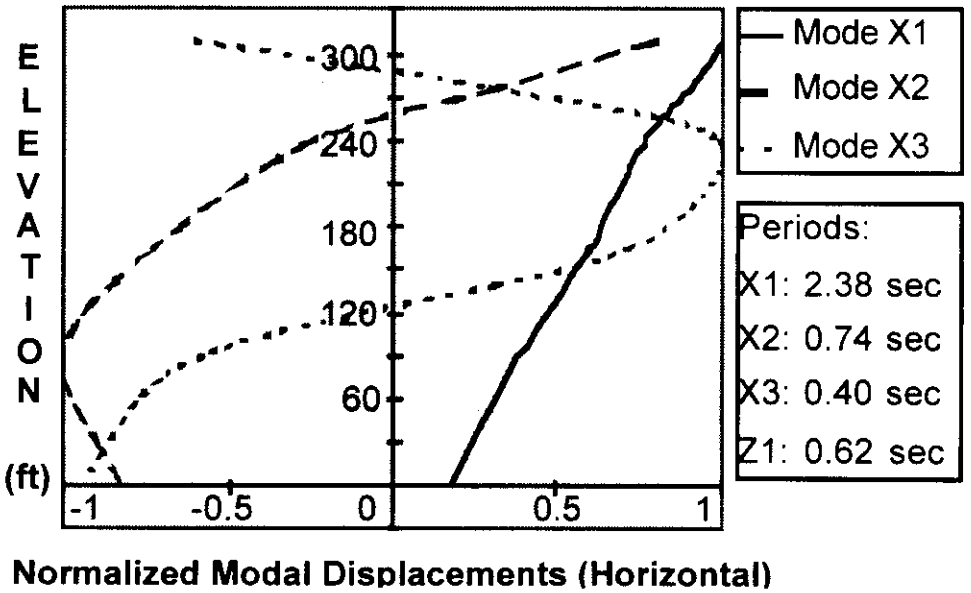

Figure 9: Platform Vibration Properties, End-On (SRSA)

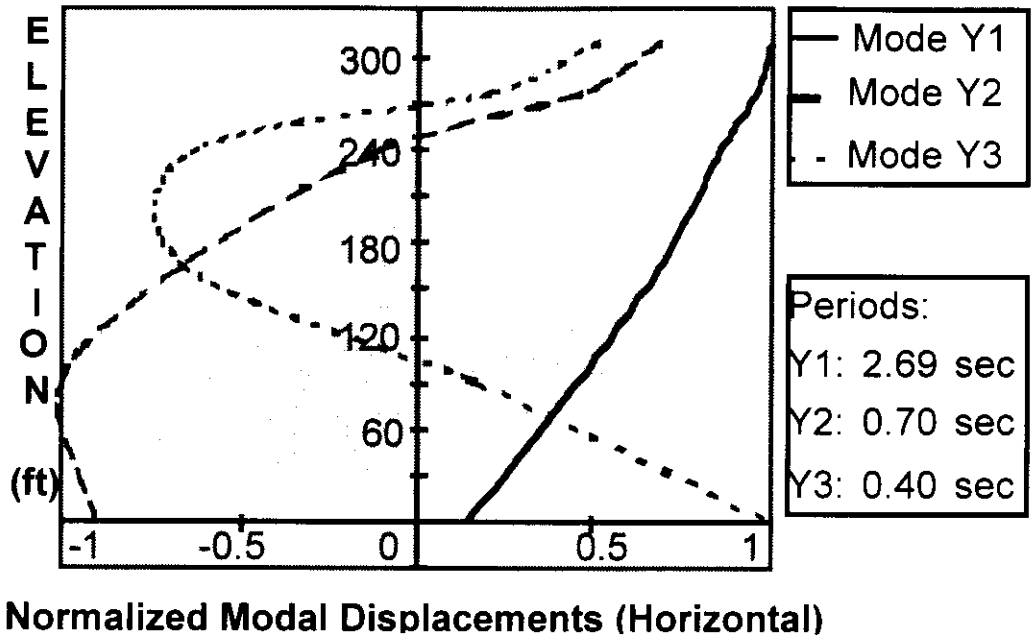

Figure 10: Platform Vibration Properties, Broadside (3-D)

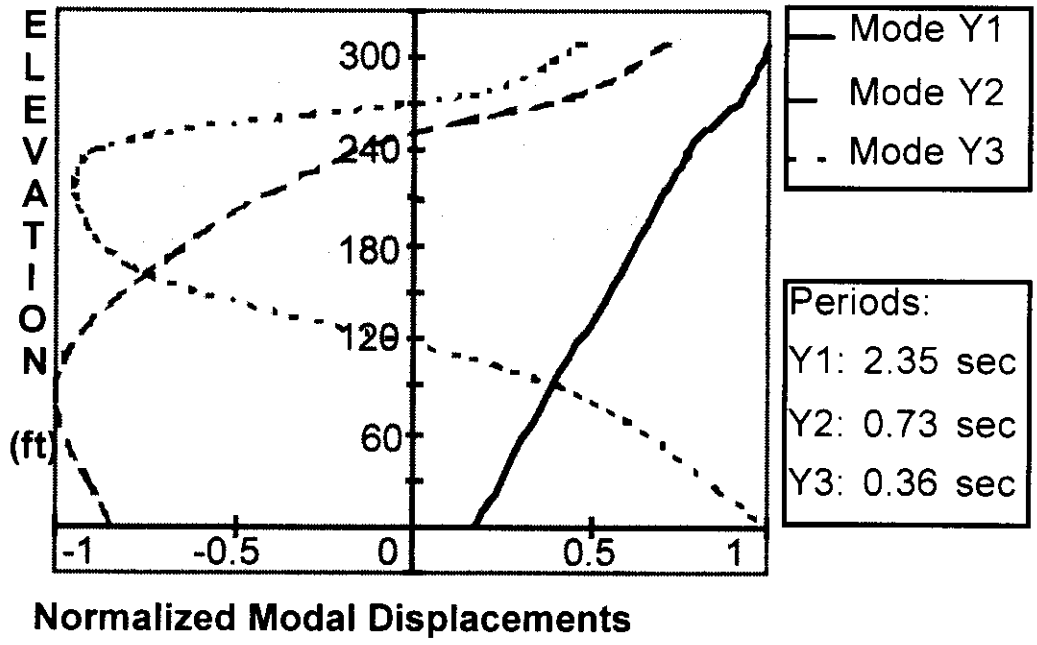

Figure 11: Platform Vibration Properties, Broadside (SRSA)

Table 5: Pile Loads on 66 in. ϕ

Pile Load	3D (kips)	Simple (kips)
Tension	4337	5034
Compression	6837	7534
Lateral	449	479

Table 6: Pile Loads on 48 in. ϕ

Pile Load	3D (kips)	Simple (kips)
Tension	1952	2522
Compression	4452	5022
Lateral	233	248

Application of the simple method indicates an earthquake intensity of 0.36 g at full strength end-on will result in yielding of the corner piles in compression. Increasing the load further results in full collapse with the failure of braces in the first jacket bay; this is achieved for an earthquake intensity of 0.42 g. For the case of full strength broadside load, the simple method indicates piles will yield at an intensity of 0.4 g, while collapse in the jacket starts in the first jacket bay for an intensity of 0.52 g. Demand - capacity diagrams for these two cases are shown below in Figures 13 and 14 (note that the foundation lateral capacities do not have the conductor strength contributions included). Using the 3-D frame model, an end-on full-strength intensity of 0.38 g was found to initiate yielding in the corner piles, while an intensity of 0.48 g resulted in the buckling of braces in the first jacket bay. For the case of full-strength broadside loading, an intensity of 0.4 g initiated pile yielding, while buckling of first bay braces occurred at an intensity of 0.55 g.

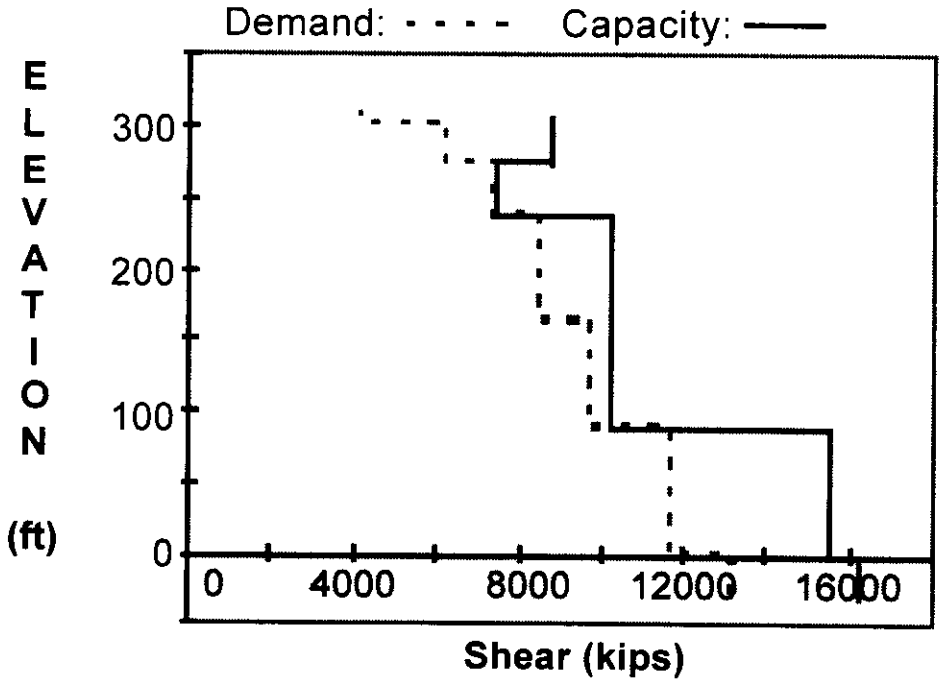

Figure 13: Demand - Capacity Profile, ULSLEA-SRSA (End-On)

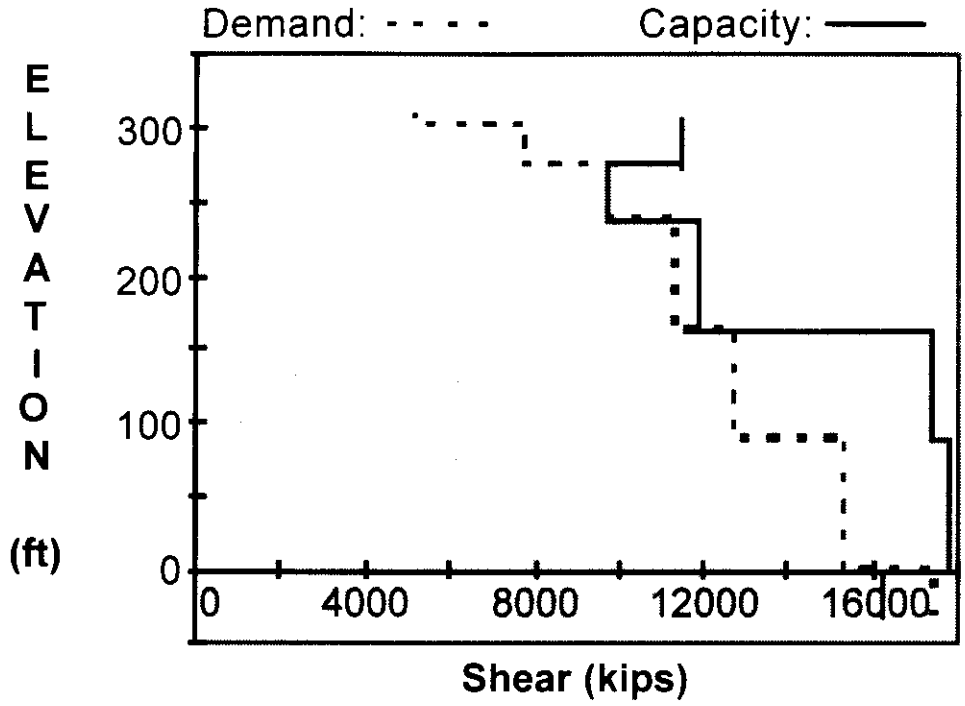

Figure 14: Demand - Capacity Profile, ULSLEA-SRSA (Broadside)

The ULSLEA-SRSA results are in good agreement with those obtained from the 3-D analysis, providing failure intensities within 15% of those obtained from the 3-D analysis.

Discussion

The simple approach to assessing platform earthquake resistance compares very well to the more rigorous 3-D frame analysis. For substantially less effort than that required for the creation and analysis of a 3-D model, excellent estimates of platform performance can still be obtained. However, it must be emphasized that the simple modal analysis procedure loses accuracy as the complexity of the structure increases, as seen by the differences in the period estimates for the 8-leg structure. While the simple results are sufficient to envelope behavior for preliminary design and initial structural integrity assessments, they would not be of great use when trying to analyze a platform for a specific earthquake (i.e. with a jagged point spectrum), due to the possible variation in structural period.

A. 5 Parameter Studies

In this section, several additional issues related to the simplified analysis of offshore platforms are explored. As an alternative to using the SRSA approach to generate earthquake force estimates, an approach based on modified Uniform Building Code (UBC, 1994) earthquake forces is reviewed. Also, several common approximate procedures for determining pile stiffnesses are compared, and the general dependence of platform response on foundation flexibility is studied. Finally, the significance of including local member forces on tubular braces is examined.

A Design Code Approach to Seismic Demands

As an alternative to rigorously evaluating the vibration properties of a platform using modal analysis and then applying the response spectrum approach, there exist several semi-empirical earthquake-demand estimating approaches such as the one contained in Chapter 16 of the Uniform Building Code (UBC, 1994). These approaches are based upon the study of general trends of structural response to earthquakes, and are intended to allow for the development of forces with which a structural design can be started.

The UBC approach for horizontal forces assumes the structure in question has no great stiffness discontinuities, and that higher mode effects will decrease rapidly in significance. A total approximate base shear is estimated, and then distributed over the height of the structure in proportion with the mass at each level. In addition, a concentrated force is applied at the top to ensure that forces from higher modes will not be neglected in the upper portions of the structure.

To evaluate the utility of this approach in estimating earthquake demands for offshore structures, the basic force estimating procedure has been adapted for use with the API response spectrum. Base shear (immediately above the foundation) is estimated from:

$$V = SA_{T_1} W \tag{22}$$

where:

SA_{T1} = pseudo-acceleration from response spectrum for fundamental period
W = total mass of the structure, not including foundation

The UBC recommends the following formula to estimate fundamental horizontal periods for braced frame structures:

$$T_1 = 0.02(h)^{0.75} \tag{23}$$

where:

h = height of structure above ground line (ft)

This period assumes no foundation flexibility, and hence will be too rigid for most offshore platforms. However, if estimates of foundation stiffnesses can be made, the fundamental period can be modified according to a period-lengthening procedure suggested by Veletsos and Boaz (1979):

$$\tilde{T}_1 = T_1 \sqrt{1 + \frac{k_1^*}{K_x}\left[\frac{1}{1-(T_o/\tilde{T}_1)^2} + \frac{K_x h_1^{*2}}{K_\vartheta}\right]} \tag{24}$$

where:

T_1 = fixed-base fundamental period
T_o = natural period of foundation mass
k_1 = effective horizontal stiffness of fixed-base fundamental
K_x = horizontal stiffness of foundation

K_θ = rotational stiffness of foundation
h_1^* = effective mass center above base, not including foundation mass

The effective horizontal stiffness can be approximated by:

$$k_1^* = \frac{4\pi^2 \left(0.9 M_1\right)}{T_1^2} \tag{25}$$

where:

M_1 = inertial mass of platform

The natural period of the foundation mass can be estimated from:

$$T_o = 2\pi \sqrt{\frac{W_o}{g K_x}} \tag{26}$$

where:

W_o = weight of foundation mass included in model
g = acceleration due to gravity

The forces distributed at the various levels in the structure are then determined in accordance with:

$$F_x = \frac{(V - F_t) w_x h_x}{\sum_{i=1}^{n} w_i h_i} \tag{27}$$

where:

F_t = $0.07VT_1$
w = mass at level
h = height of level

F_t is applied at the top of the structure, in addition to F_x at the top level. To obtain an estimate of the shear imposed on the foundation, the maximum base shear V found above is combined with an approximate value of the inertia force of the foundation mass (Veletsos, Boaz, 1979):

$$V_o = \left(\left(\frac{W_o A_o}{g} \right)^2 + V^2 \right)^{0.5} \tag{28}$$

where:

A_n = pseudo-acceleration of the foundation mass calculated from the response spectrum

To evaluate the utility of this modified UBC approach, it has been applied to the analysis of both Platform A and Platform B from the previous section. Earthquake shears determined from 3-D response spectrum analysis (the SRSS rule was used to combine modes) are shown together with shears estimated by the modified UBC approach in Figures 15 and 16. The same pile and conductor stiffnesses used in the previous section were used to develop foundation translation and rotation stiffnesses.

For Platform A, the shears found using the UBC approach agree quite well with those found through application of 3-D RSA, being within 6% of the RSA values. The fundamental period estimate is quite good, 1.44 sec compared to 1.47 sec from 3-D modal analysis. For Platform B, the results are less in agreement. The periods estimated using the UBC approach are low for both primary directions of load (2.23 sec vs. 2.89 for end-on, and 2.28 sec vs. 2.69 sec for broadside). Consequently, the estimated shears are higher, in some instances by as much as 25%.

The modified UBC approach provides another simple method of obtaining demands on a platform for preliminary design or initial structural assessment purposes. However, it must be recognized that the approach will tend to under-predict the periods of large structures, leading to associated changes in predicted load dependent upon the response spectrum.

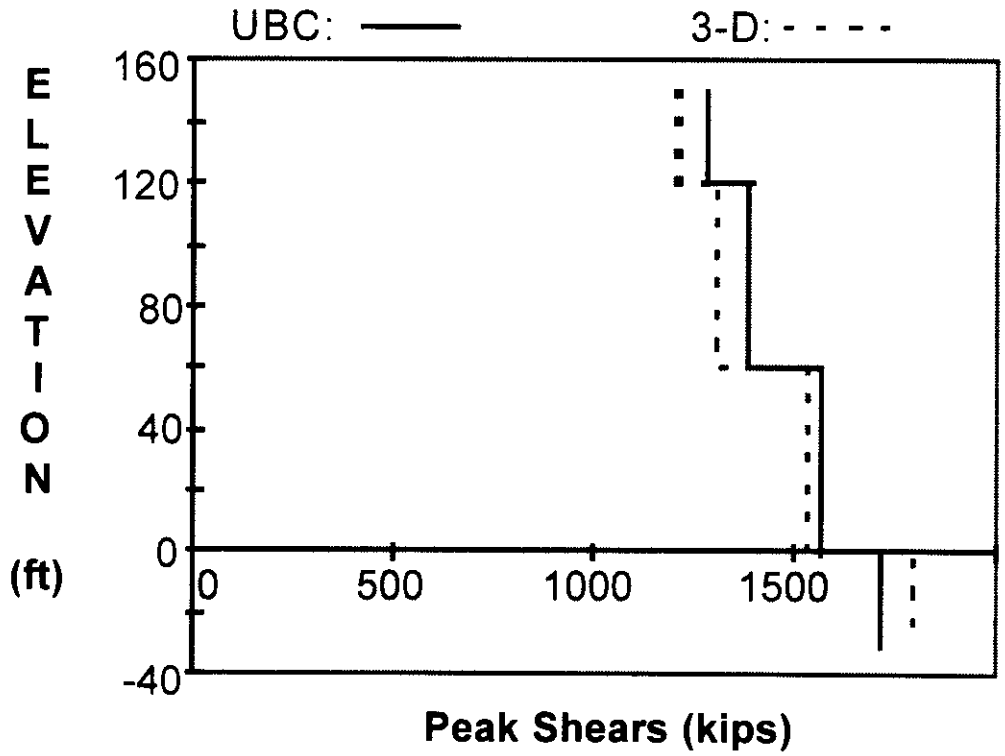

Figure 15: Comparison of UBC Forces and 3-D Modal Analysis Forces, Platform A

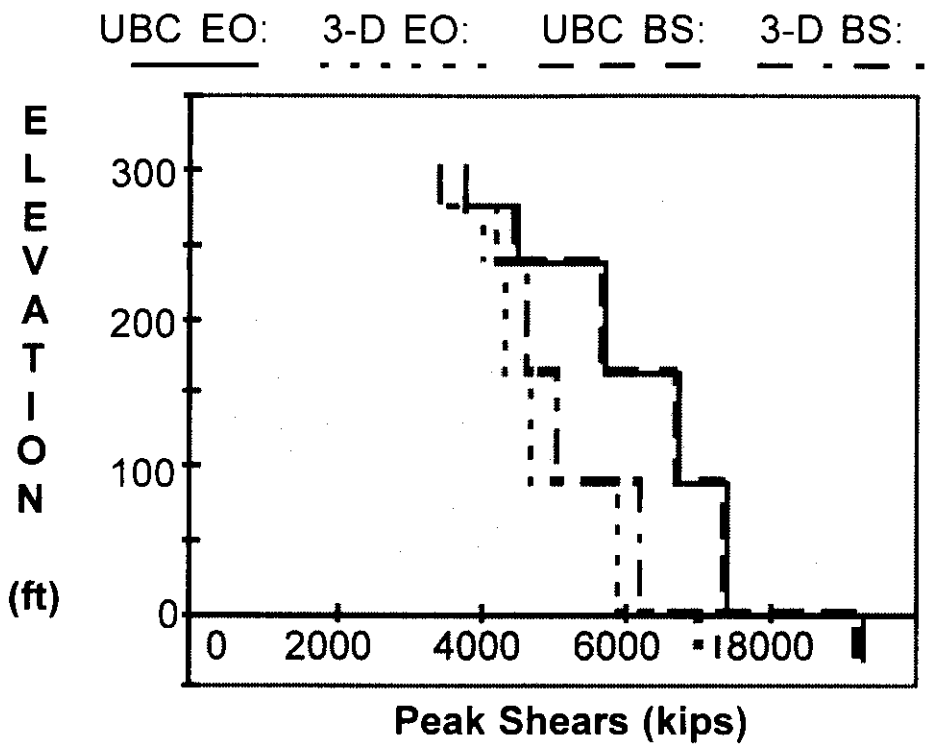

Figure 16: Comparison of UBC Forces and 3-D Modal Analysis Forces, Platform B

Foundation Stiffness

As the foundation is a significant source of platform flexibility, it is important that the associated stiffness properties of the foundation be well represented. Typically, the stiffness contributions of mud mats and mudline braces are ignored, while stiffnesses for piles and conductors are developed by modeling the pile as a segmented beam supported by springs, and then developing pile-head load-deflection behavior from these models. Developing pile-head behavior using this approach can be quite time-consuming.

In lieu of using the above procedure, a number of approximate approaches are available to estimate pile-head stiffnesses. Perhaps the most common approach to estimating lateral pile-head stiffnesses is to consider the pile to be a beam fixed at the mudline and fixed at some depth L (between five and ten pile diameters) below the mudline:

$$k_x = \frac{12EI}{L^3} \tag{29}$$

An alternative for pile-head horizontal stiffness is that used by Penzien (1975) in a series of studies of offshore platforms subjected to earthquakes:

$$k_x = 18.2Gr\frac{(1-\upsilon^2)}{(2-\upsilon)^2} \tag{30}$$

where:

G = shear modulus of the foundation soil
υ = Poisson's ratio for the foundation soil
r = pile radius

This horizontal stiffness k_x is derived using elastic half-space theory and assuming the pile is deeply imbedded. Unless the foundation is extremely soft, the horizontal loads will be transferred quite rapidly to the surrounding soil with depth. Hence, the horizontal stiffness of each pile can be derived by considering the pile-head to be a rigid circular footing supported on an elastic medium. It is assumed to connection between the pile and jacket is rigid and allows for no pile-head rotation.

Pile-head vertical stiffnesses are often estimated by considering the basic stiffness *EA/L* of the pile column and then modifying this stiffness for the mechanism by which vertical loads are transferred to the surrounding soil. Various transfer mechanisms are shown in Figure 17.

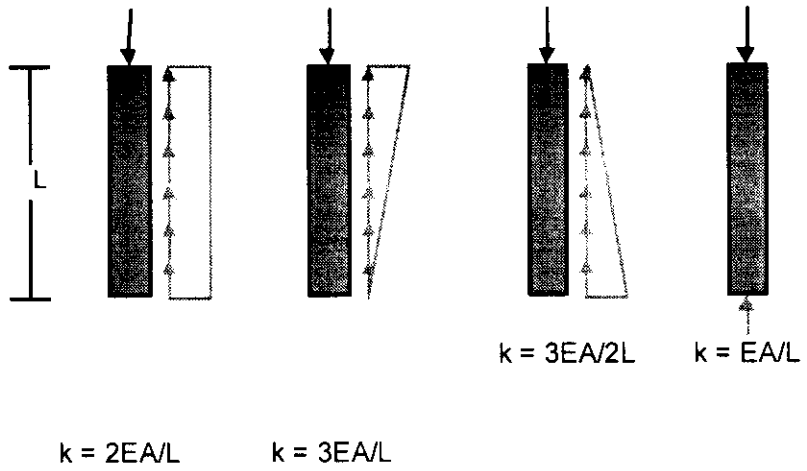

Figure 17: Vertical Load Transfer Mechanisms for Imbedded Piles

Another approach to estimating pile head stiffnesses is that suggested by Dobrey (1980). These approximations are based on previous work by Novak (1974) and Blaney, et al. (1976). Assuming foundation strength to rely upon soil elastic modulus and assuming as a basis a beam on an uniform elastic foundation, pile-head stiffnesses take the form:

$$k_z = 0.8\frac{E_p A}{r}\left(\frac{E_s}{E_p}\right)^{0.5} \tag{31}$$

$$k_x = 2\frac{E_p I}{r^3}\left(\frac{E_s}{E_p}\right)^{0.75} \tag{32}$$

$$k_\theta = 1.6\frac{E_p I}{r}\left(\frac{E_s}{E_p}\right)^{0.25} \tag{33}$$

$$k_{\theta x} = -1.2\frac{E_p I}{r^2}\left(\frac{E_s}{E_p}\right)^{0.5} \tag{34}$$

where:

E_p = Elastic modulus of pile material
E_s = Elastic modulus of soil material
I = Moment of inertia of pile steel cross-section

Assuming there is no applied moment at the pile head, the effective horizontal stiffness can be represented by:

$$k_{x\,\text{effective}} = k_x - \frac{k_{\theta x}^2}{k_\theta + k_{\theta\,\text{structure}}} \tag{35}$$

This effective stiffness will vary depending on the amount of rotational stiffness supplied by the structure attached to the pile head, $k_{\theta\,structure}$. These formulas are intended for intermediate values of E_s/E_p, and r/L ratios in the range of 10 to 50.

A comparison has been made between the various approximate pile-head stiffness and those derived during the course of the two example platform analyses described in the previous section. Pile-head stiffnesses from the different approximations along with those used in the examples are shown below in Tables 7 and 8:

Table 7: Horizontal Pile-Head Stiffnesses (kips/in)

Diameter (in.)	$12EI/L^3$ L=5D	$12EI/L^3$ L=10D	Penzien kx	Dobry kx	3-D kx
72	1093	136	870	515	469
66	1640	205	598	623	260
48	1640	205	435	623	135

Table 8: Vertical Pile-Head Stiffnesses (kips/in)

Diameter (in.)	3EA/L	EA/L	Dobry kz	3-D kz
72	10933	3644	2915	3150
66	8541	2847	3787	4496
48	7069	2356	3787	2825

There is much variation between the approximate methods and the springs derived for the 3-D analyses. However, it must be remembered that these estimates can be obtained with much less effort than constructing and analyzing a segmented pile model. Furthermore, given the fact that soil properties can possess significant biases due to sampling and testing methods, there will be an element of variation to the springs derived from detailed analyses; this must be recognized by the analyst. The best of action when making use of these approximations is to select sets which will provide upper and lower bounds on the stiffnesses.

To study the effect of foundation flexibility on the horizontal response of a platform, the axial and horizontal pile-head stiffnesses used with Platform A and Platform B were varied with respect to the values calculated from the detailed analysis (see Tables 6 and 7). The variation in fundamental horizontal period for both Platforms are shown below in Figures 18 and 19. Varying the stiffnesses for Platform A can change the period by as much as 33%. This could have a significant effect on calculated loads, depending upon the response spectrum being used. For Platform B, the maximum variation is 14%. This is less significant, and is due to the larger flexibility of the un-grouted 8-leg jacket. Nevertheless, it is important to recognize that there can be significant variation in the pile stiffnesses due to factors beyond the control of the analyst.

To study the general impact of these forces, both Platform A and Platform B were analyzed using the simple approach with the local inertia forces set to zero. Demand - capacity profiles for both platforms are shown in Figure 20, Figure 21 and Figure 22, with capacities derived both with and without local forces. For Platform A, the effect of the local inertia forces is small. However, many members in Platform B are strongly affected by the presence of these forces. This difference is due to the fact that many members in the lower bays of Platform B are very long, even though they possess similar cross section properties to those members in Platform A. Figures 21 and 22 make clear the necessity of including these local forces in design considerations; several members in Platform B have their axial capacities reduced on the order of 38 %.

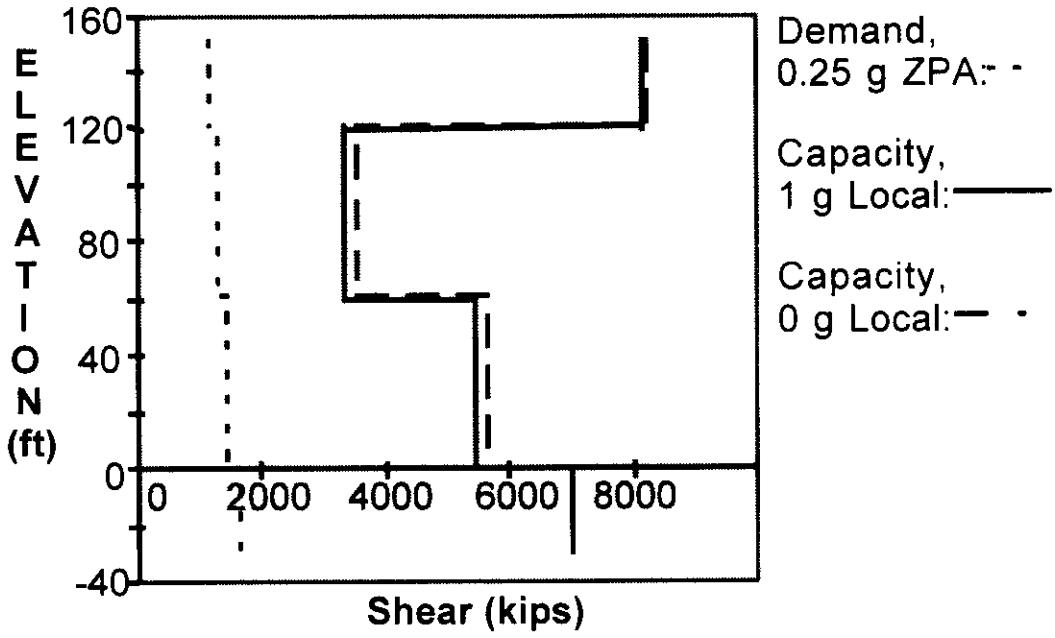

Figure 20: Platform A

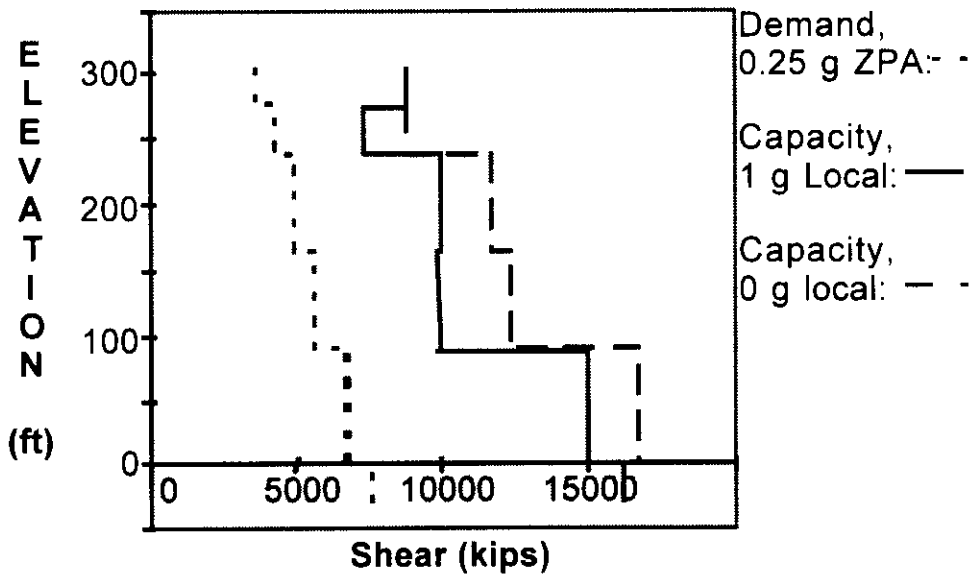

Figure 21: Platform B, End-On

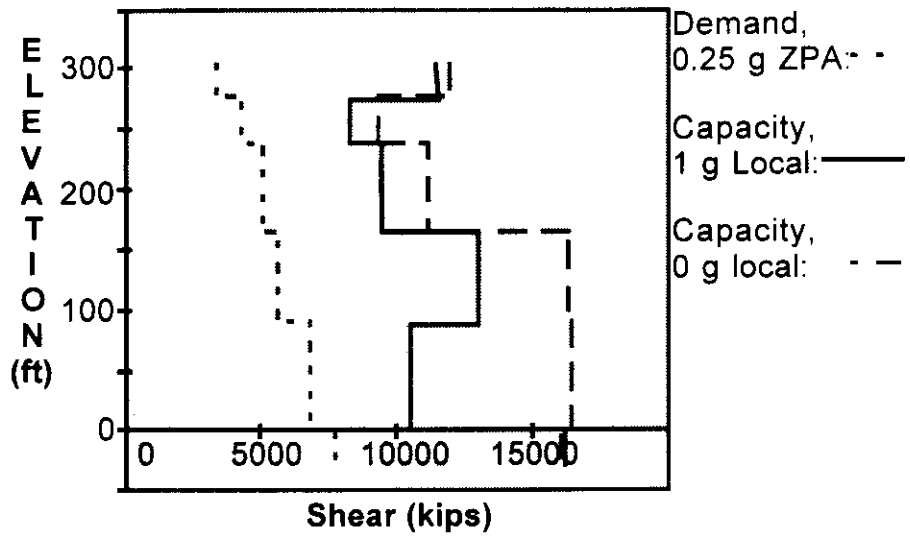

Figure 22: Platform B, Broadside

A.6 Observations and Conclusions

The ULSLEA-SRSA earthquake assessment approach described within the first section provides results which are in very good agreement with those obtained from more rigorous analysis effort. The approach does, however, have limitations when applied to complicated structures, especially those which have no grout between the jacket legs and piles. For the cases studied, ULSLEA-SRSA was able to provide earthquake failure intensities (spectrum ZPA for the API response spectrum when load pattern indicates first member failure) for strength-level evaluations within 15 % of those estimated using 3-D frame analysis. It must be noted, however, that vibration periods estimated by the simple approach tend towards being low compared to periods estimated using a more-complete model; while the observed variation did not effect loads much this should be taken into account when using spectra where the higher period range sees the greatest excitation. Given that the simple approach requires much less effort than that involved in performing a 3-D frame analysis, it is ideally suited to performing preliminary design studies and preliminary assessments of existing structures

The modified UBC approach was demonstrated to be another satisfactory method by which estimates of horizontal forces can be obtained for a platform in lieu of performing a 3-D frame analysis. This approach provides an excellent starting point to the estimation of earthquake forces for a strength-level design.

Reviewing some approximations to pile-head stiffnesses, it was seen that there was wide variation in the estimated stiffnesses as compared to the results of more detailed modeling. However, it must be recognized that there can be substantial variation in true pile performance due to uncertainties in the properties of the surrounding soil. Therefore, attempts should be made to obtain upper and lower bounds on pile stiffnesses, in order to obtain a range in expected behavior of the attached platform. It should be noted that most current modeling practice for these platforms do not account for mud mat and mudline brace contributions to foundation stiffness; past experience (Ruhl, 1976; Bannon, Penzien, 1992) has indicated that many platforms behave as though they are fixed at the bottom, due

to contact between the jacket and sea floor. While it is possible that softening could taken place for the soils beneath these mudline elements, the possibility of actually possessing a significantly stiff foundation should be considered when performing an analysis.

Finally, the relative significance of local forces on long, unsupported tubular members was qualitatively examined. It was demonstrated that for some large bracing members, the effective axial capacity can be reduced by as much as 30 % by the presence of local inertia forces. It is imperative that these forces not be neglected when performing an analysis.

A.7 References

American Petroleum Institute (1993). *Recommended Practice for Planning, Designing and Constructing Fixed Offshore Platforms - Load and Resistance Factor Design*, API Recommended Practice 2A-LRFD (RP 2A-LRFD), 1st Edition, Washington, D. C.

Bannon, H., and Penzien, J. (1992). "Working Group Report on Structural Performance," *Proceedings of the International Workshop on Seismic Design and Reassessment of Offshore Structures*, editor: W. D. Iwan, California Institute of Technology, Pasadena, CA.

Bea, R. G., and Mortazavi, M. (1995). "Simplified Evaluation of the Capacities of Template-Type Offshore Platforms," *Proceedings of the 5th International Offshore and Polar Engineering Conference*, The Hague, The Netherlands.

Bea, R. G., Mortazavi, M. M., Loch, K. J., and Young, P. L. (1995). "Verification of a Simplified Method to Evaluate the Capacities of Template-Type Platforms," *Proceedings of the Offshore Technology Conference*, OTC 7780, Houston, TX.

Blaney, G. W., Kausel, E., and Roesset, J. M. (1976). "Dynamic Stiffness of Piles," *Proceedings of the 2nd International Conference on Numerical Methods in Geomechanics*, ASCE, Blacksburg, VA.

Bowen, C. M. and Bea, R. G. (1995). "Simplified Earthquake Floor Response Spectra for Equipment on Offshore Platforms," *Proceedings of the International Workshop on Wind and Earthquake Engineering for Coastal and Offshore Facilities*, Department of Civil Engineering, University of California at Berkeley, CA.

Clough, R. W. (1960). "Effects of Earthquakes on Underwater Structures," *Proceedings of the 2nd World Conference on Earthquake Engineering*, Tokyo.

Dobry, R., Vicente, E., and O'Rourke, M. (1980). "Equivalent Spring and Damping Coefficients for Individual Piles Subjected to Horizontal Dynamic Loads," paper submitted for publication in the *Journal of the Geotechnical Division*, ASCE.

Goyal, A., and Chopra, A. K. (1989). *Earthquake Analysis and Response of Intake-Outlet Towers*, Report No. UCB/EERC-89/04, Earthquake Engineering Research Center, University of California at Berkeley, CA.

Mortazavi, M. (1995). *A Probabilistic Screening Methodology for Use in Assessment and Requalifications of Steel, Template-Type Offshore Platforms*, Ph.D. Dissertation, Department of Civil Engineering, University of California at Berkeley, CA.

Mortazavi, M. and Bea, R. G. (1997). "Experimental Validation of the Ultimate Limit State Equilibrium Analysis (ULSLEA) with Results from Frame Tests," *Proceedings of the 7th International Offshore and Polar Engineering Conference*, Honolulu, Hawaii.

Novak, M. (1974). "Dynamic Stiffness and Damping of Piles," *Canadian Geotechnical Journal*, Vol. 11, No. 4.

Penzien, J. (1975). "*Seismic* Analysis of Platform Structure-Foundation Systems," *Proceedings of the Offshore Technology Conference*, OTC 2352, Houston, TX.

Ruhl, J. A. (1976). "Offshore Platforms: Observed Behavior and Comparisons with Theory," *Proceedings of the Offshore Technology Conference*, OTC 2553, Houston, TX.

Stear, J. D., and Bea, R. G. (1997). "Evaluating Simplified Analysis Approaches for Estimating the Load Capacities of Gulf of Mexico Jacket-Type Platforms," *Proceedings of the 16th International Conference on Offshore Mechanics and Arctic Engineering*, Yokohama, Japan.

Uniform Building Code (1994).

Veletsos, A. S., and Boaz, I. B. (1979). "Effects of Soil-Structure Interaction on Seismic Response of a Steel Gravity Platform," *Proceedings of the Offshore Technology Conference*, OTC 3404,